Time-Resolved ESR Studies on Fragmentation of Initiators and Initiation Step in Photopolymerization

1. Introduction

1.1 Radical polymerization

In addition polymerization of vinyl monomers, radical photopolymerization is frequently used as well as ionic one.[1)] The process of radical polymerization consists of an initiation step, a propagation step and a termination step. An initiator radical is formed by fragmentation of initiator and addition reaction of monomer occurs in the initiation step. The polymer chain propagates by addition of monomer in the propagation step. The propagation of polymer chain terminates due to recombination or disproportionation between terminal radicals each other in the termination step. Photofragmentation of initiator occurs in the photopolymerization case. The reactions of photopolymerization are shown in Scheme (1.1). The simplest mechanism is presented here for radical polymerization. The chain transfer, the termination due to the initiator radicals and the other reactions are neglected in the present system.

In the steady-state irradiation of light, radical polymerization continues under steady-state concentrations of radicals. These conditions can be represented as

$$d[R\cdot]/dt = R_f - k_i[M][R\cdot] = 0 \qquad (1.1.a)$$

$$[R\cdot] = R_f/k_i[M] \qquad (1.1.b)$$

$$d[M\cdot]/dt = k_i[M][R\cdot] - 2k_t[M\cdot]^2 = 0 \qquad (1.2.a)$$

$$[M\cdot] = (k_i[M][R\cdot]/2k_t)^{1/2} = (R_f/2k_t)^{1/2}, \qquad (1.2.b)$$

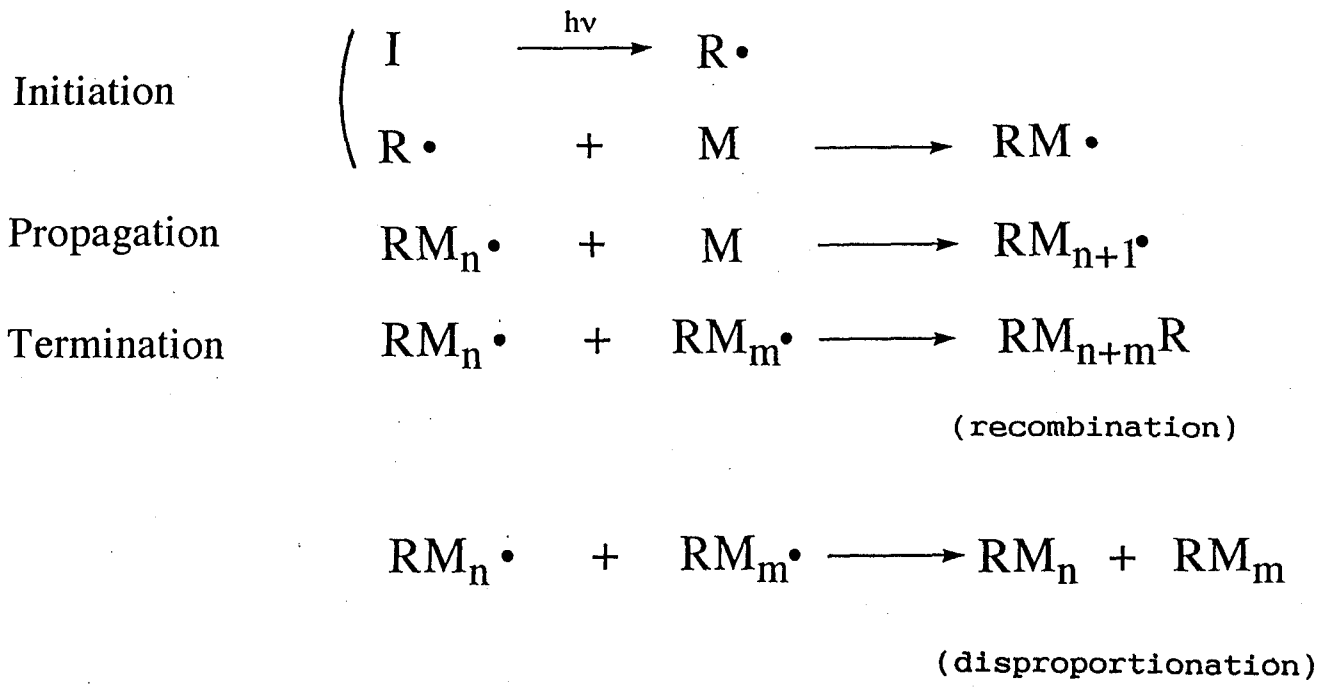

Scheme (1.1) Reactions of photopolymerization system.

where R_f is the photofragmentation rate of initiator, k_i, k_p and k_t are the rate constant of addition to the initiator radical, the rate constant of propagation and termination of polymer radical respectively. The values of k_p and k_t are assumed to be independent of radical size. The term of [M·] represents the sum of the concentrations of the propagating chain radicals. The photofragmentation rate of initiator R_f is proportional to the intensity of irradiation and the concentration of initiator. The polymerization rate, that is, the propagation rate R_p, is

$$R_p = -d[M]/dt = k_p[M\cdot][M]$$
$$= k_p(R_f/2k_t)^{1/2}[M]. \qquad (1.3)$$

The rate constant of termination k_t is usually much larger than that of propagation k_p, because termination is due to reaction between active radicals. The polymer radical, however, can sufficiently propagate, because the monomer concentration [M] is much larger than the radical concentration [M·].

The kinetic chain length ν, which is the ratio of the rate of propagation to the rate of initiation or termination, can be represented as

$$\nu = R_p/R_i = k_p[M\cdot]/k_i[R\cdot]$$
$$= R_p/R_t = k_p[M]/(2k_tR_f)^{1/2}. \qquad (1.4)$$

If the chain transfer is absent, the kinetic chain length is proportional to the molecular weight of polymer. The average degree of polymerization is ν, when the termination is due to

disproportionation only. The average degree of polymerization is 2ν, when the termination is due to recombination perfectly. In general the average degree of polymerization is between ν and 2ν.

When the termination due to the initiator radical is considerable, the kinetics of radicals is represented as

$$d[R\cdot]/dt = R_f - k_i[M][R\cdot] - k_t'[M\cdot][R\cdot] - 2k_t''[R\cdot]^2 \qquad (1.5)$$

$$d[M\cdot]/dt = k_i[M][R\cdot] - 2k_t[M\cdot]^2 - k_t'[M\cdot][R\cdot], \qquad (1.6)$$

where k_t' is the rate constant of termination between the initiator radical and one of the propagating radicals, while k_t'' is for termination between the initiator radicals. The termination reaction is dependent on diffusion of molecules, because the reaction occurs in encounter of radicals. Thus, the values of k_t' and k_t'' are larger than k_t in general. Because of the small size, the initiator radical can diffuse more easily than the propagating radicals. In the simplest case described above, however, the concentration of monomer is much larger than the initiator radical, so that the addition of monomer is dominant in reactions of the initiator radical. Then, the third and fourth terms are negligible in equation (1.5). In these consideration of the kinetics of initiator radical, the value of k_i is significant. The value of k_i is determined by noting the addition of monomer, that is, the initiation reaction in the present studies. In equation (1.6), the third term is negligible in the steady-state where $[R\cdot] \ll [M\cdot]$, as well as equation (1.5).

Radical polymerization is carried out in several methods. Bulk polymerization is carried out without other solvent. The initiator is dissolved in monomer as solvent in bulk polymerization. Solution polymerization is carried out where the initiator and the monomer are dissolved in other solvent. Suspension polymerization is carried out where the monomer exists as oil droplets in the aqueous phase. The initiator is dissolved in monomer droplets in suspension polymerization. On the other hand, the monomer exists as emulsion in the aqueous phase and radical polymerization is carried out with the initiator which can be dissolved in the aqueous phase, such as $K_2S_2O_8$, in emulsion polymerization. Although emulsion polymerization shows the different kinetics, bulk polymerization, solution polymerization and suspension polymerization occur according to the same kinetics described above. In the present studies, the experiments for polymerization systems were carried out under the condition of solution or bulk polymerization.

1.2 Esr studies on radical polymerization

Fischer et al. reported the esr studies on the polymerization by redox initiators with the flow-mixing method for acrylic acid, methacrylic acid, methylmethacrylate and other monomers.[2)] At low concentrations of monomer, the esr spectrum of monomer radical is observed. The spectra of polymer radicals are observed as the monomer concentration increase. The spectra of these radicals can be discriminated one another, because of the hyperfine structure (hfs). Fischer et al. discussed the conformation of propagating radicals.

Ranby et al. also reported the esr studies on the redox polymerization of vinylacetate and other monomers with the flow-mixing method.[3] The spectrum of monomer radical is observed at high concentrations of monomer in comparison with acrylic acid and methylmethacrylate. The stability of propagating radicals was discussed. In the presence of a second monomer, Ranby et al. observed the copolymer radicals of vinylacetate and other monomers and studied the copolymerization system by the esr method.[4]

In those studies, the initiation step of polymerization was observed with the esr method. The primary propagating radical, which is formed by addition of monomer to the initiator radical, is detected. Those esr studies, however, were carried out with the flow-mixing method, so that the conditions are different from the real polymerization systems. Furthermore, the systems are almost all the thermal-redox polymerization which occured in the aqueous solution.

The esr studies on photopolymerization were reported with the continuous-flow method of solution by Smith et al.[5] The esr observations were carried out in the photolysis of azocompounds as initiator under the steady-state irradiation. The esr spectrum of initiator radical is observed in the absence of monomers. In the presence of monomer, which is alkyl methacrylates, methacrylonitrile or styrene, the esr spectrum of the propagating polymer radicals is observed and the signal intensity of initiator radical is decreased. The terminal conformation of polymer radicals was discussed from esr signals. According to Smith et al., however, the fraction of the primary propagating radical is small in

the steady-state system of photopolymerization. Since the observed spectrum of propagating radicals is independent of initiators, they have concluded that the observed spectrum is due to the polymerized propagating radicals including several monomer units. Although the spectrum of the primary propagating radical is different from that of the polymerized propagating radicals, no esr spectrum is observed except for the initiator radical and the polymer radicals. The primary propagating radical from the initiation reaction is not observed under their conditions.

Smith et al. discussed the radical-size distribution F_x in the kinetic analysis of polymerization system.[5a,5c,5d] In the steady state where the termination due to the initiator radical can be neglected, the kinetic chain length ν is given by equation (1.4). In this case, the radical-size distribution is given by

$$F_x = [RM_x\cdot]/[M\cdot] = \nu^{-1}(1+\nu^{-1})^{-x}, \qquad (1.7)$$

where $[RM_x\cdot]$ is the concentration of the polymer radical including x monomer units. The fraction of the primary propagating radical is given by

$$F_1 = [RM_1\cdot]/[M\cdot] = (1+\nu)^{-1}. \qquad (1.8)$$

Smith et al. estimated F_1 with available ν in the photopolymerization system of methylmethacrylate under their experimental conditions.[5a] The result of estimation supports that the fraction of the primary propagating radical is very small. In their experiments, however, the discussion on the details of polymeri-

zation kinetics is difficult, because of the uncertainty of the radical concentrations.[5d)]

The esr studies on the propagating radicals in the steady-state polymerization were also reported by Bresler et al.[6)] The esr observations were carried out in the homogeneous polymerization by thermal initiation for styrene, methylmethacrylate and vinylacetate. In this case, the spectra of propagating radicals are observed and radical concentration is estimated from esr signals. The values of k_p and k_t were calculated according to the kinetics of polymerization.

Kamachi et al. studied the terminal conformations of propagating radicals under UV irradiation with the esr method by using of the TM110 cavity.[7)] The spectra of several propagating radicals were observed in the steady state. The kinetic studies on polymerization were also carried out and the solvent effect on k_p is found in solution polymerization. In case of low k_t due to the steric effect of radicals, the esr spectra of propagating radicals are observed with usual TE011 cavity in the polymerization of several monomers.[7)] Especially, the primary propagating radicals are observed in the polymerization of di-butyl itaconate initiated by azocompounds.

In those esr studies on the steady-state polymerization, the propagating radicals of polymer are mainly observed. The conformation of radical terminal and the kinetic parameters of polymerization are discussed from esr experiments.

1.3 Chemically Induced Dynamic Electron Polarization (CIDEP)

The radicals observed by the time-resolved esr method show emission or enhanced absorption of signals due to chemically induced dynamic electron polarization (CIDEP) in most cases.[8] The population of electron spin is different from the thermal equilibrium state in CIDEP. The populations of the thermal equilibrium state and the CIDEP are shown in Figure (1.1).

When intersystem crossing ocurrs from the singlet state to the triplet state in the excited molecule, the difference in the rates of intersystem crossing generates spin polarization in the triplet sublevels. Thus, the radicals formed from the polarized triplet state within the spin conservation show the CIDEP signal. The CIDEP signal due to the triplet mechanism (TM) shows a total-emission or a total-absorption of spectrum, because the relative intensity is determined by multiplicity of individual line in the spectrum. In the case of total-absorption, the CIDEP signal due to the TM is hardly distinguished from that of the thermal equilibrium state by the spectral pattern.

The interaction between radicals in a radical pair also generates spin polarization. The CIDEP signal due to the radical pair mechanism (RPM) shows the dependence on the hyperfine state of the radical. When the radicals are formed from the triplet precursor (T-precursor), the radicals show the emission/absorption (E/A) pattern of spectra. When the radical are formed from the singlet precursor (S-precursor), they show the absorption/emission (A/E) pattern of spectra. The spin polarization due to the RPM is generated in free pairs (F-pair) of radicals, which is formed in encounter of free radicals. The CIDEP signal shows the E/A pattern of spectra in the case of F-

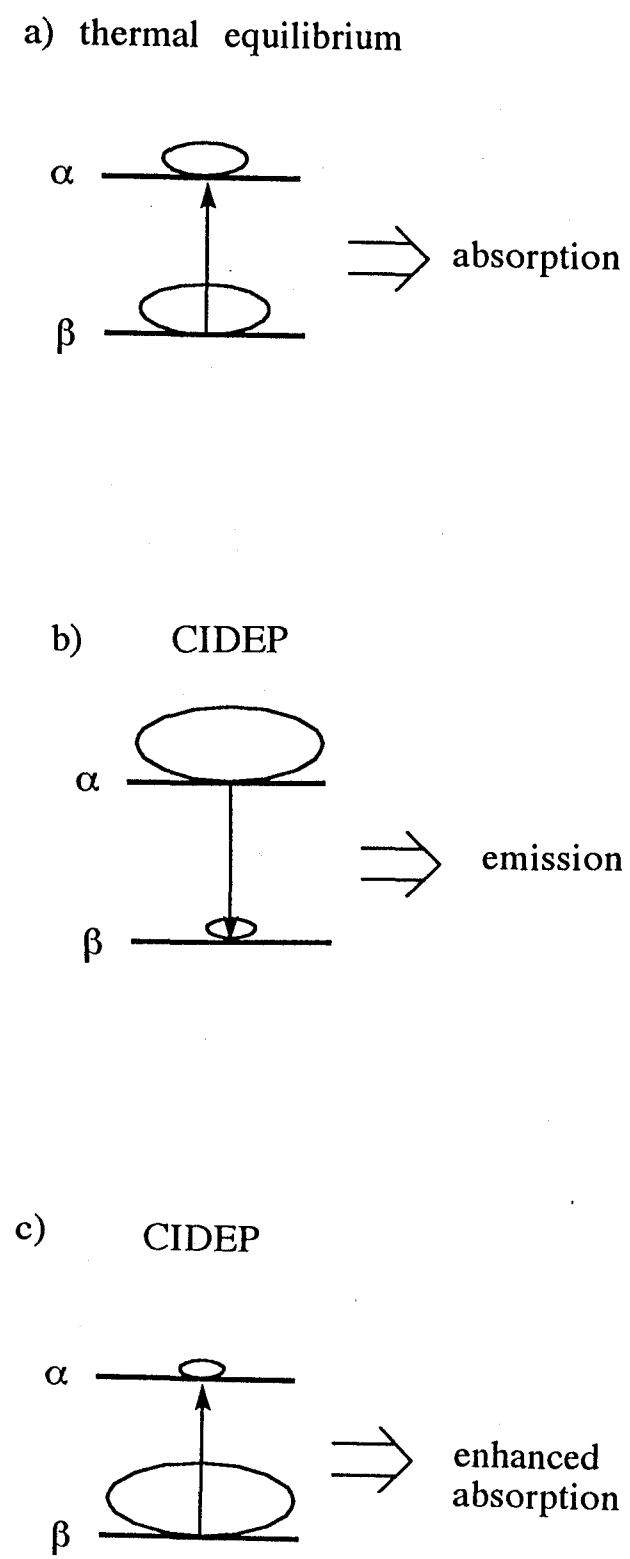

Figure (1.1) Population of electron spin. a) thermal equilibrium (Esr signal shows absorption.) b) CIDEP (emission) c) CIDEP (enhanced absorption)

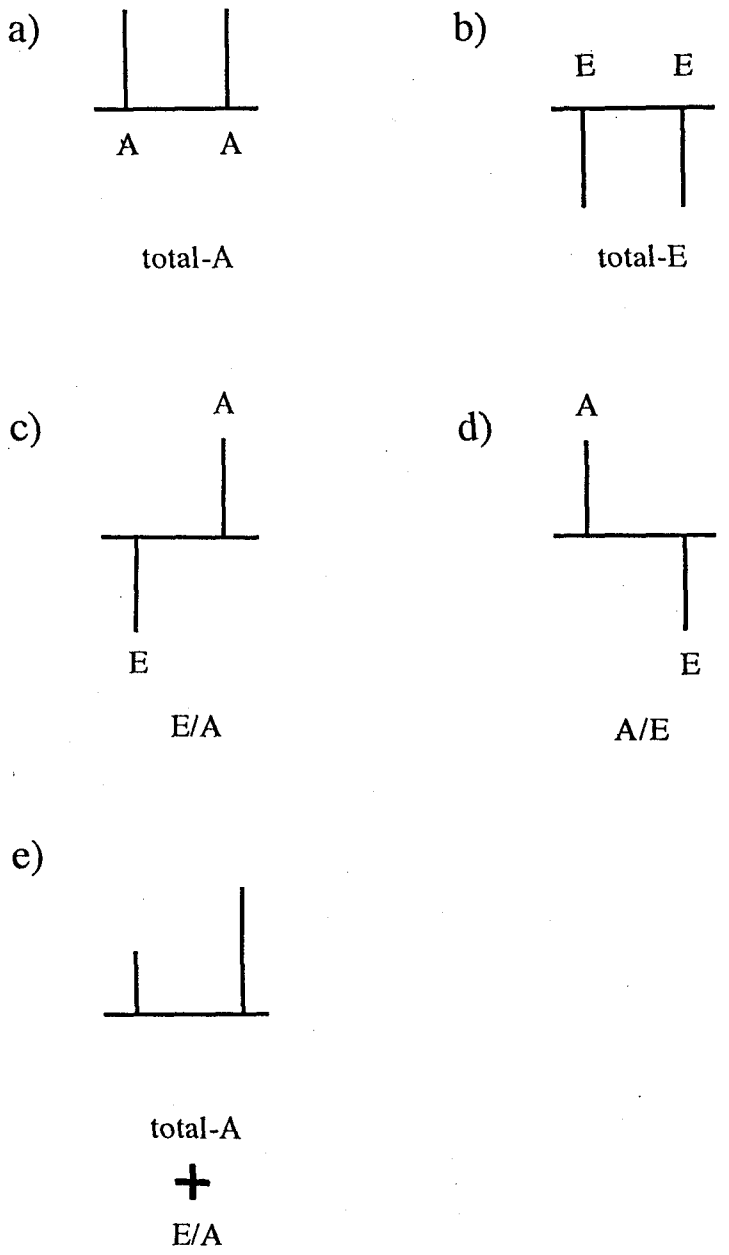

Figure (1.2) CIDEP patterns of esr spectrum which shows the hfs due to a nucleus (I=1/2). a) total-absorption (total-A) due to the TM, b) total-emission (total-E) due to the TM, c) emission/absorption (E/A) due to the RPM in case of triplet-precursor, d) absorption/emission (A/E) due to the RPM in case of singlet-precursor, e) superposition of a) total-A and c) E/A.

pair. For example, the spectral patterns of CIDEP are shown in Figure (1.2) for the radical which shows the hfs due to a nucleus (I=1/2), such as a phosphorus nucleus. In case of radicals from the T-precursor, the CIDEP signal occationally shows superposed spectral patterns due to the TM and the RPM.

The CIDEP signal shows the decay due to the spin-lattice relaxation.[9] The spin polarization relaxes to the thermal equilibrium state. The decay of CIDEP is induced by the application of microwave. Thus, the decay rate of CIDEP signal is dependent on microwave power. The dependence on the microwave power is an evidence that the observed signal is due to CIDEP and its decay is not caused by chemical reactions but the CIDEP decay.

1.4 Acylphosphine compounds as initiators of photopolymerization

In photocuring of polymer resins, acylphosphine compounds are used as initiator of polymerization.[10] Investigations have been reported on polymerization by using of acylphosphine oxide as initiator.[11,12] The typical compound is 2,4,6-trimethyl benzoyldiphenylphosphine oxide (TMDPO) which was most frequently studied. The diphenylphosphinoyl radical and the 2,4,6-trimethylbenzoyl radical are formed in the photofragmentation of TMDPO, as shown in Scheme (1.2). These transient radicals initiate the polymerization of vinyl monomer.

The di-*o*-tolylphosphinoyl radical and the 2,4,6-trimethylbenzoyl radical are formed in the photofragmentation of di-*o*-tolyl-2,4,6-trimethylbenzoylphosphine oxide (TMTPO). Either the 2,4,6-trimethylbenzoyl radical and the diphenylthiophosphinoyl radical or the di-*o*-tolyl-thiophosphinoyl radical, are formed in

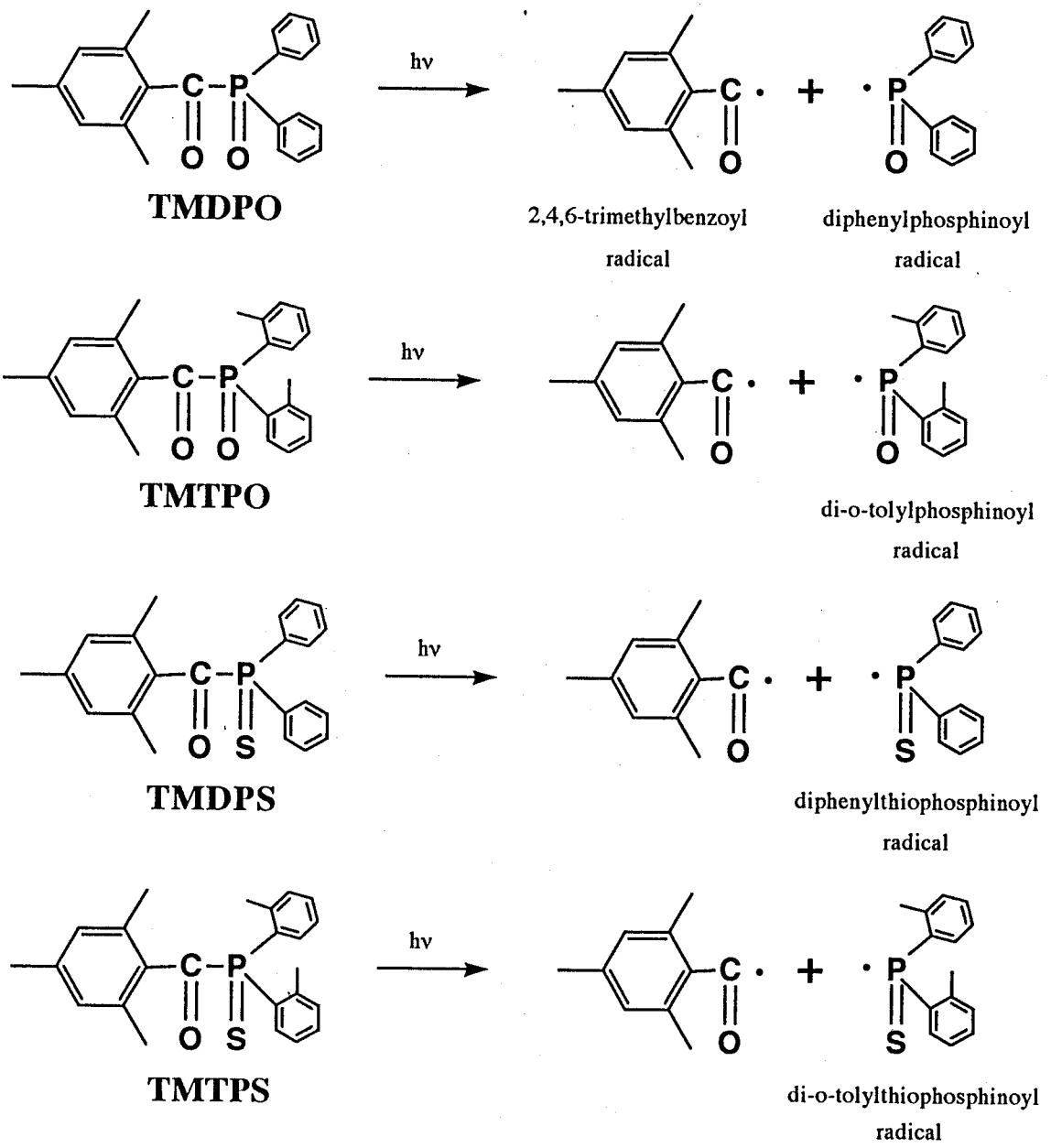

Scheme (1.2) Photofragmentation of acylphosphine compounds. TMDPO, TMTPO, TMDPS, TMTPS and the fragment radicals.

the photofragmentation of acylphosphine sulphides, which are 2,4,6-trimethylbenzoyldiphenylphosphine sulphide (TMDPS) and di-*o*-tolyl-2,4,6-trimethylbenzoylphosphine sulphide (TMTPS). The photofragmentations of these compounds are shown in Scheme (1.2). These transient radicals also initiate the polymerization of the vinyl monomer.

Previous investigations on the acylphosphine compounds are mentioned later. In the present work, the initiation step of photopolymerization is studied by using of the acylphosphine compounds as initiator.

1.5 Purpose of the present work

In the previous esr studies on polymerization, the observation of initiation step was restricted to the redox-initiation system in aqueous solutions with the flow-mixing method. The spectra of the primary propagating radicals were observed in the dilute concentration of monomer or in case of the specific monomers. On the other hand, the esr studies were carried out on the conformation of polymer radicals and the kinetics of polymerization in the steady-state system of polymerization.

The purpose of the present work is the esr observation of *the initiation step* in photopolymerization, which consists of the photofragmentation of the initiator and the addition of the monomer to the initiator radical. The time-resolved esr method is applied to the photopolymerization system. Transient initiator radicals are observed on the photofragmentation of initiators by the time-resolved esr method. The contribution of CIDEP is discussed on the observed signals of initiator radicals. The real-

time observation is carried out on the addition of the monomer to the initiator radical. The primary propagating radical is observed in a nonaqenous system at relatively high concentrations of monomer. The rate constant of initiation k_i is directly determined from the decay of esr signals. The time-resolved measurement, CIDEP and the specific photoinitiator, that is, the acylphosphine compounds enabled the present studies.

References to chapter 1

1. (a) P.J.Flory, Principles of Polymer Chemistry, Cornell University Press, New York, (1953).
   (b) G.Oster and N.Yang, Chem. Res., 68, 125(1968).
2. (a) H.Fischer, J. Polym. Sci., B2, 529(1964).
   (b) H.Fischer, Makromol. Chem., 98, 179(1966).
   (c) H.Fischer and G.Giacometti, J. Polym. Sci., C16, 2763(1967).
3. (a) H.Yoshida and B.Ranby, J. Polym. Sci., C16, 1333(1967).
   (b) K.Takakura and B.Ranby, J. Polym. Sci., A-1, 8, 77(1970).
4. (a) K.Takakura and B.Ranby, J. Polym. Sci., B5, 83(1967).
   (b) K.Takakura and B.Ranby, J. Polym. Sci., C22, 939(1969).
5. (a) P.Smith and R.Stevens, J. Phys. Chem., 76, 3141(1972).
   (b) P.Smith, L.B.Gilman and R.A.DeLorenzo, J. Magn. Reson., 10, 179(1973).
   (c) P.Smith, R.D.Stevens and L.B.Gilman, J. Phys. Chem., 79, 2688(1975).
   (d) P.Smith, L.B.Gilman, R.D.Stevens and C.Vignola de Hargrave, J. Magn. Reson. 29, 545(1978).
6. (a) S.E.Bresler, E.N.Kazbekov, V.N.Fomichev and V.N.Shadrin, Makromol. Chem., 157, 167(1972).
   (b) S.E.Bresler, E.N.Kazbekov and V.N.Shadrin, Makromol. Chem., 175, 2875(1974).
7. M.Kamachi, Adv. Polym. Sci., 82, 207(1987), Springer-Verlag Berlin Heidelberg, and references therein.
8. (a) J.K.S.Wan, S.Wong and D.A.Hutchison, Acc. Chem. Res.,7, 58(1974).
   (b) J.K.S.Wan and A.J.Elliot, Acc. Chem. Res., 10, 161(1977).

(c) P. J. Hore, C. G. Joslin and K. A. McLauchlan, Chem. Soc. Rev., 8, 29(1979).

(d) C. D. Backley and K. A. McLauchlan, Mol. Phys., 54, 1(1985).

(e) K. A. McLauchlan and D. G. Stevens, Acc. Chem. Res., 21, 54(1988).

(f) J. H. Freed and J. B. Pedersen, Adv. Mag. Resonance, 8, 2(1976), Academic Press.

(g) L. Kevan and R. N. Schwartz(editor), Time Domain Electron Spin Resonance, Wiley-Interscience (1979).

9. (a) P. W. Atkins, K. A. McLauchlan and P. W. Percival, Mol. Phys., 25, 281(1972).

(b) P.J.Hore and K.A.McLauchlan, J. Magn. Reson. 36, 129(1979).

10. A.Jacobi and A.Henne, J. Radiat. Curing, 10(4), 16(1983).

11. (a) J.E.Baxter, R.S.Davidson and H.J.Hageman, Eur. Poly. J., 24, 419(1988).

(b) J.E.Baxter, R.S.Davidson and H.J.Hageman, Eur. Poly. J., 24, 551(1988).

(c) J.E.Baxter, R.S.Davidson, M.A.U.de Boer, H.J.Hageman and P.C.M. van Woerkom, Eur. Poly. J., 24, 819(1988).

(d) J.E.Baxter, R.S.Davidson and H.J.Hageman, Polymer, 29, 1569(1988).

(e) J.E.Baxter, R.S.Davidson, H.J.Hageman and T.Overeem, Makromol. Chem., 189, 2769(1988).

12. (a) Y.Yagci and W. Schnabel, Makromol. Chem. Symp., 13/14, 161(1988).

(b) Y.Yagci, J.Borebely and W.Schnabel, Eur. Polym. J., 25,

129(1988).

2. Experimental

2.1 Time-resolved esr spectroscopy

Time-resolved esr spectroscopy is useful for the investigation of transient radicals in photochemical systems. The time profiles of esr signal can be obtained.[1)] The brock diagram of a time-resolved esr system is shown in Figure (2.1). The time-resolved esr measurement is carried out without magnetic field modulation, because of the fast signal observation. At fixed magnetic field point, the time profile of esr signals is recorded in a trnsient recorder after laser irradiation which feeds a trigger pulse to the recorder, as shown in Figure (2.2). The signal is accumulated in a microcoputer. The magnetic field sweep and the laser irradiation are controled by the microcomputer. A time-resolved esr spectrum can be constructed by time integration of signal profiles over the entire range of the spectrum in the microcomputer.[1e,1f)]

The signal acquisition after laser irradiation can be also carried out with a boxcar integrator, as shown in Figure (2.2). In this case, the laser irradiation is controled by the trigger signal of a pulse generater. Time-resolved esr spectrum is obtained by the field-sweep observation.

2.2 Materials

The acylphosphine compounds (TMDPO, TMTPO, TMDPS and TMTPS) were obtained from BASF. The solvents (benzene, *n*-dodecane, *n*-hexane and toluene) purchased from Wako Pure Chemical Industries, Co. Ltd. were used without further purification. 4-Amino-2,2,6,6- tetramethylpiperidinyl-1-oxy (ATEMPO) pur-

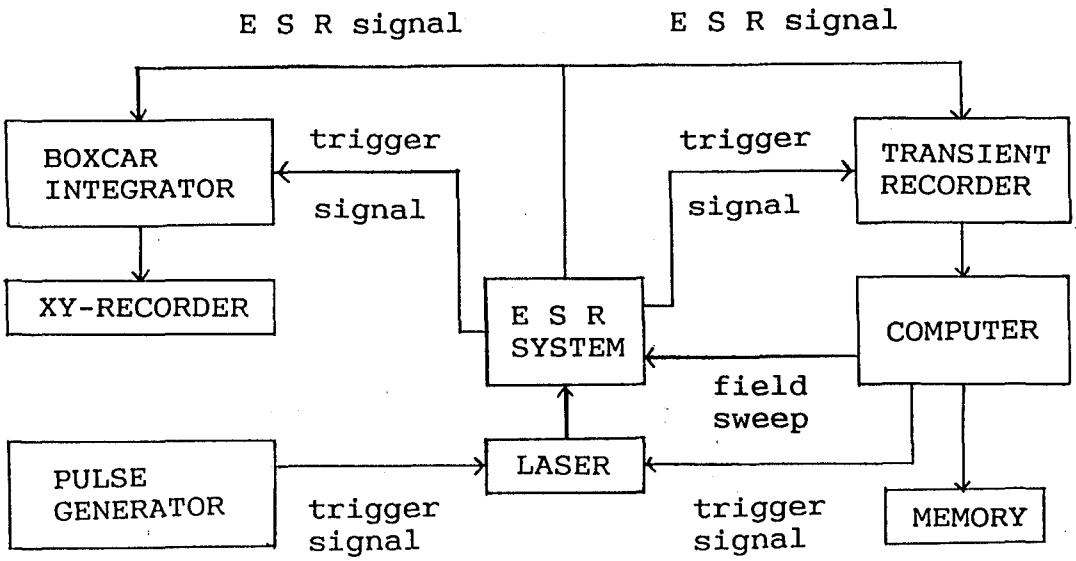

Figure (2.1) Block diagram of time-resolved esr system. Signal acquisition is carried out by transient recorder or boxcar integrator.

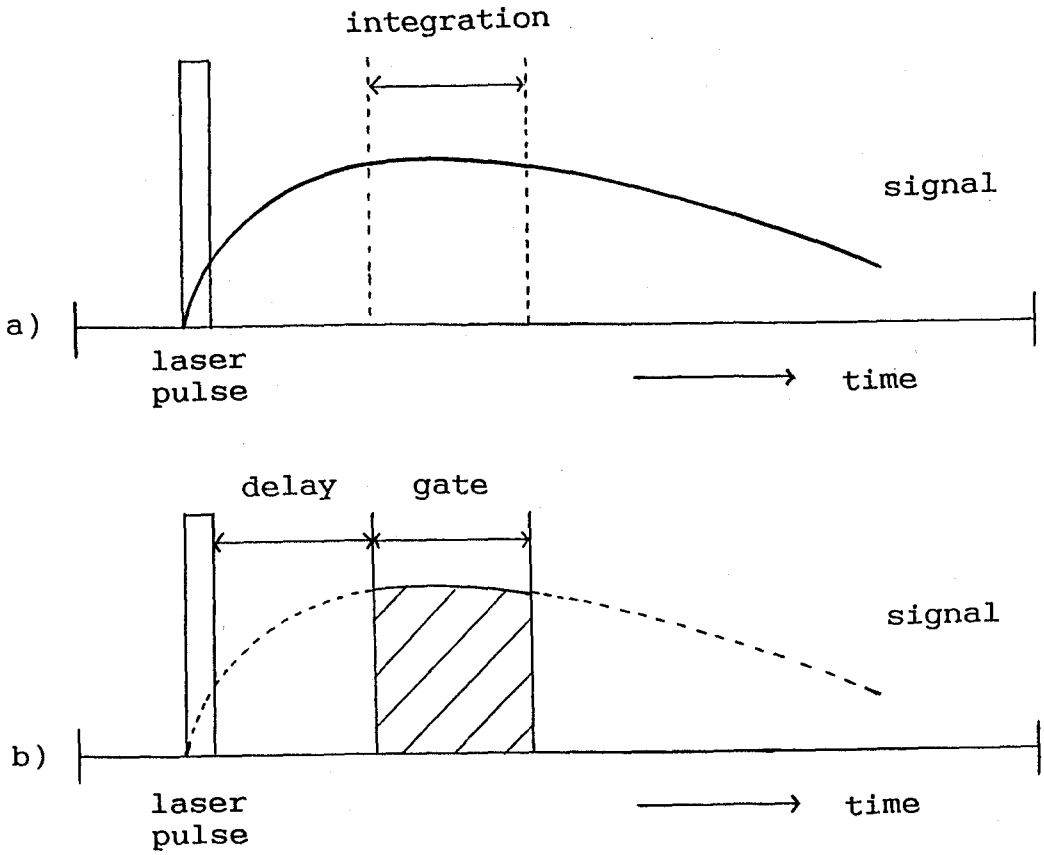

Figure (2.2) Observation of signal in time-resolved esr spectroscopy. a) time profile of signal with transient recorder at fixed magnetic field point. b) Signal acquisition with boxcar integrator.

chased from Sigma Chemical Company was used without further purification. Naphthalene and tris(acetylacetonate) chromium (III) ($Cr(acac)_3$) purchased from Wako Pure Chemical Industries, Co. Ltd. were used without further purification. α-Methylstyrene (αMS) purchased from Tokyo Kasei Kogyo, Co. Ltd. was washed with aqueous solution of sodium hydroxide (20%), dried by calcium hydrides, and distilled under vacuum. Methylmethacrylate (MMA) purchased from Wako Pure Chemical Industries, Co. Ltd. was distilled. 2,2'-Azobisisobutyronitrile (AIBN) purchased from Wako Pure Chemical Industries, Co. Ltd. was used without further purification.

2.3 Samples and esr measurements

Sample solutions were prepared by dissolving the acylphosphine compounds with other reagents in benzene. The concentration of the acylphosphine compounds was 0.1 mol dm^{-3}. The concentrations were ATEMPO 0.05 mol dm^{-3}, naphthalene 1 to 4 mol dm^{-3}, and $Cr(acac)_3$ 0.001 to 0.004 mol dm^{-3}, respectively. The concentration of olefinic compounds was 0.025 to 1.0 mol dm^{-3}. Furthermore, the measurements of the *n*-dodecane and the *n*-hexane solutions of TMTPS were carried out.

The sample solutions of the acylphosphine compounds were degassed under vacuum and irradiated with laser pulses in a quartz cell (thickness of 5 mm) in a TE011 mode esr cavity. In the case of oxygen effect, the sample was oxygenated by bubbling of the oxygen gas for 3 minutes and irradiated in the cell. The samples were irradiated with an excimer laser (XeCl: wavelength of 308 nm) in the experiment of ATEMPO. In other cases, the

samples were irradiated with nitrogen laser (wavelength of 337 nm). The time-resolved esr measurements were carried out at room temperature by an X-band ESR spectrometer without magnetic field modulation. Time profiles of esr signal after irradiation were recorded in a transient memory of 10 ns sampling time (Iwatsu, Co. Ltd. DM901). The digitized data were sent to a microcomputer (NEC PC9801VX) and accumulated for 30 laser pulses. The accumulated time profile of esr signals was obtained at a fixed magnetic field point. The off-resonance signal was substructed from each time profiles in the microcomputer. The measurements of time profiles were carried out at different field points with a fixed interval of the magnetic field. Time-resolved field-swept esr spectra were constructed by time integration of the time profiles over 200 ns period in the microcomputer.[2)]

A toluene solution and an MMA solution of AIBN were prepared at the concentration of 0.2 mol dm^{-3}. In neat MMA, the concentration of MMA is 9.5 mol dm^{-3}. The solutions of AIBN (ca. 200 dm^3) were deoxygenated by bubbling of the nitrogen gas and circulated through a quartz flow cell (thickness of 1 mm) in the esr cavity. The samples were irradiated with an eximer laser (XeF: wavelength of 351 nm) at room temperature. A boxcar integrator was used to record the field-swept esr spectra over 200 ns period by 200 ns after a laser pulse. Then, the magnetic field was swept over the entire range of esr spectra.[3)]

References to chapter 2

1. (a) R.W.Fessenden, J. Chem. Phys., 58, 2489(1973).
   (b) N.C.Verma and R.W.Fessenden, J. Chem. Phys., 65, 2139(1976).
   (c) S.S.Kim and S.I.Weissman, J. Magn. Reson., 24, 167(1976).
   (d) A.D.Trifunac, M.C.Thurnauer and J.R.Norris, Chem. Phys. Lett., 57, 471(1978).
   (e) S.Basu, K.A.McLauchlan and G.R.Sealy, J. Phys. E: Sci. Instrum., 16, 767(1983).
   (f) K. A. McLauchlan and D. G. Stevens, Acc. Chem. Res., 21, 54(1988).
2. M.Kamachi, K.Kuwata, T.Sumiyoshi and W.Schnabel, J. Chem. Soc. Perkin Trans 2, 961(1988).
3. T.Takemura, K.Ohara, H.Murai and K.Kuwata, Chem. Lett., 1635(1990).

3. Analysis of esr signal decays by modified Bloch equations

In the time-resolved esr investigations, the time evolution of esr intensity can be analyzed by the modified Bloch equations, in which the initial spin polarization and chemical reactions are considered. The time dependent solutions of the Bloch equations have been given analytically on resonance. Time profiles of the intensity on resonance have been reconstructed according to the analytic solutions.[1-6)]

The monomer concentration hardly changes with reactions in the present study, because it is much larger than that of the fragment radicals of the initiator. A pseudo-first-order reaction of the fragment radical with the monomer molecules is considered. Then, the Bloch equations include the first-order reaction terms. The equations in the rotating system on resonance may be written as

$$dM_x(t)/dt = -T_2^{-1}M_x(t) - k_1M_x(t) \qquad (3.1.a)$$

$$dM_y(t)/dt = -T_2^{-1}M_y(t) - \omega_1M_z(t) - k_1M_y(t) \qquad (3.1.b)$$

$$dM_z(t)/dt = \omega_1M_y(t) - T_1^{-1}M_z(t) - k_1M_z(t) + n(t)T_1^{-1}P_{eq} \qquad (3.1.c)$$

$$dn(t)/dt = -k_1n(t), \qquad (3.1.d)$$

where notations have usual meanings.[3)] The n(t) term represents the concentration of the radical at time t and decreases according to the first-order kinetics. The rate constant k_1 is the sum of pseudo-first-order rate constants, such as the rate constant

of addition reaction of the monomer molecule. In these equations, the generation of spin polarization due to the RPM of the F-pair is assumed to be negligible. Although the decay curves of signal were distorted by the F-pair, it is not dominant in the present system. Thus, the terms from the F-pair can be omitted in the equations, in order to analyze the dominant decay of signals.

These equations can be solved analytically by Laplace transformation. The analytic solutions of the equations have been reported.[1,3,4] The intensity of signal is given by the y-component of magnetization,

$$M_y(t) = \frac{\omega_1}{r_+ + r_-}\{ [m_0 + \frac{T_1^{-1}P_{eq}n_0}{k_1 + r_-}]\exp(r_-t) - [m_0 + \frac{T_1^{-1}P_{eq}n_0}{k_1 + r_+}]\exp(r_+t) - \frac{T_1^{-1}P_{eq}n_0(r_+ - r_-)}{(k_1 + r_+)(k_1 + r_-)}\exp(-k_1t) \}, \quad (3.2)$$

$$r_\pm = -1/2[1/T_1^* + 1/T_2^*] \pm [1/4(1/T_2^* - 1/T_1^*)^2 - \omega_1^2]^{1/2} \quad (3.3)$$

where $1/T_1^* = 1/T_1 + k_1$ and $1/T_2^* = 1/T_2 + k_1$. In equation (3.2), m_0 is the initial value of the z-component of magnetization, that is, the initial spin polarization, and n_0 is the ini-

tial radical concentration, respectively. The initial conditions of equations (3.1) are $M_x(0) = M_y(0) = 0$, $M_z(0) = m_0$, and $n(0) = n_0$.

If $(1/T_2^* - 1/T_1^*)^2 >> 4\omega_1^2$ and $1/T_2^* >> 1/T_1^*$ are satisfied, equations (3.3) can be written as $r_- \sim -1/T_2^*$ and $r_+ \sim -(1/T_1^* + T_2\omega_1^2)$, respectively.[1] The former condition means that microwave power is sufficiently weak. (ω_1^2 is proportional to the microwave power of observation.) The latter means that T_2 is much shorter than T_1. These conditions are easily satisfied in several cases. Thus, equation (3.2) becomes

$$M_y(t) = T_2\omega_1\{ m_0\exp(-t/T_2^*) - [m_0 - \frac{P_{eq}n_0}{1 + T_1T_2\omega_1^2}]\exp(-[1/T_1^* + T_2\omega_1^2]t) - \frac{P_{eq}n_0}{1 + T_1T_2\omega_1^2} \exp(-k_1t) \}. \quad (3.4)$$

In the present study, the decay curves of the esr signal are discussed according to equation (3.4). In equation (3.4), the first term corresponds to the rise of signal and the second term represents the exponential decay of the CIDEP signal to the thermal equilibrium state due to the spin-lattice relaxation and chemical reactions. The third term represents the exponential decay of the thermal equilibrium signal due to first-order reactions. Then, from the Bloch equations, it is indicated that the signal shows double exponential decay curve in the presence

of first-order chemical reactions under the conditions of $(1/T_2^* - 1/T_1^*)^2 >> 4\omega_1^2$ and $1/T_2^* >> 1/T_1^*$. The decay rate of the second term usually depends on the microwave power of observation.

In the present system, the signal showed the single exponential decay and the decay rate was not dependent on microwave power.[7] The time profile can be reproduced by equation (3.4) in the following three cases.

(1) The first is the thermal equilibrium case. The observed signal is at the thermal equilibrium in the initial state. This condition can be represented as $m_0 \sim P_{eq}n_0/(1 + T_1T_2\omega_1^2)$. In this case, the second term of equation (3.4), that is, the $\exp(-[1/T_1^* + T_2\omega_1^2]t)$ term, is vanished by cancellation. Then, the time profile of signal is written as

$$M_y(t) = \frac{T_2\omega_1 P_{eq}n_0}{1 + T_1T_2\omega_1^2}\{ \exp(-[1/T_2 + k_1]t) - \exp(-k_1t) \}. \quad (3.5)$$

The signal at thermal equilibrium decays according to the first-order chemical reactions and the decay curve shows the single exponential.

(2) The second is the fast reaction case, that is $k_1 >> 1/T_1 + T_2\omega_1^2$. The second term and the third term of equation (3.4) give the same exponential curve due to $r_+ \sim -(1/T_1 + k_1 + T_2\omega_1^2) \sim -k_1$ in the fast reaction case. Thus, equation (3.4) can be also changed into a simple form,

$$M_y(t) = T_2\omega_1 m_0\{ \exp(-[1/T_2 + k_1]t) - \exp(-k_1 t) \}. \quad (3.6)$$

The decay of signal shows the single exponential curve due to a fast chemical reaction.

(3) It is the third case that the decay of signal includes not only chemical reactions but also the spin-lattice relaxation process. Two conditions are required for this case. It is one condition that the thermal equilibrium signal is negligible in comparison with spin polarization, that is, $m_0 >> P_{eq}n_0/(1 + T_1T_2\omega_1^2)$. The other condition is $k_1, 1/T_1 >> T_2\omega_1^2$, which gives $r_+ \sim -(1/T_1 + k_1 + T_2\omega_1^2) \sim -(1/T_1 + k_1)$. (In this case, the value of k_1 is comparable with $1/T_1$. If $k_1 >> 1/T_1$, the decay curve is represented by the second case.) The time profile of signal is written as

$$M_y(t) = T_2\omega_1 m_0\{ \exp(-[1/T_2 + k_1]t) - \exp(-[1/T_1 + k_1]t) \}. \quad (3.7)$$

The former condition is required for the single exponential decay and the latter condition is required for being independent of microwave power.

In the three cases of equation (3.5) to equation (3.7), the second exponential terms of these equations represent the single exponential decay of the signal. The signal decay is due to only chemical reactions in the first and the second case. In the third case, however, the signal decay is due to both chemical reactions and the spin-lattice relaxation.

References to Chapter 3

1. P.W.Atkins, K.A.McLauchlan and P.W.Percival, Mol. Phys. 25, 281(1972).
2. N.C.Verma and R.W.Fessenden, J. Chem. Phys. 58, 2501(1973).
3.(a) J.B.Pedersen, J. Chem. Phys. 59, 2656(1973).
   (b) J.H.Freed and J.B.Pedersen, Adv. Mag. Resonance, 8, 2(1976), Academic Press.
4. N.C.Verma and R.W.Fessenden, J. Chem. Phys. 65, 2139(1976).
5. P.J.Hore and K.A.McLauchlan, J. Magn. Reson. 36, 129(1979).
6. P.J.Hore and K.A.McLauchlan, Mol. Phys. 42, 533(1981).
7. M.Kamachi, K.Kuwata, T.Sumiyoshi and W.Schnabel, J. Chem. Soc. Perkin Trans 2, 961(1988).

4. Photofragmentation of initiators

4.1 Photofragmentation of acylphosphine compounds

Investigations were carried out on the photofragmentation of the acylphosphine compounds so far. The photofragmentation of TMDPO has been studied by product analysis.[1-4] The products due to the fragment radicals have been detected. The diphenylphosphinoyl radical and the 2,4,6-trimethylbenzoyl radical are formed by type I cleavage of TMDPO, as shown in Scheme (1.2). In the transient absorption experiments, the diphenylphosphinoyl radical is detected and the contribution of the triplet excited state is observed in the photofragmentation of TMDPO.[1,5]

The time-resolved esr spectra of these radicals have been observed in the photolysis of TMDPO.[6,7] The diphenylphosphinoyl radical shows a total-absorptive spectrum, which consists of two esr lines at high field and low field due to the hfs of a phosphorus nucleus. The high field line more intense than the low field line is concluded that a weak E/A pattern superimposed on the total-absorptive spectrum. The 2,4,6-trimethylbenzoyl radical shows a broad absorptive line with no hfs at central field. The observed spectra are shown in Figure (4.1).

The esr signals show the decay in the time range of submicrosecond. The decay rate is not dependent on the microwave power of observation.[7] The decay does not reflect the spin-lattice relaxation induced by microwave. The signal decay can occur due to chemical reactions as well as the decay of CIDEP. Thus, the evidence of total-absorptive CIDEP due to the TM has not been established in the photolysis of TMDPO, because the total-absorptive CIDEP is hardly discriminated from that of the thermal

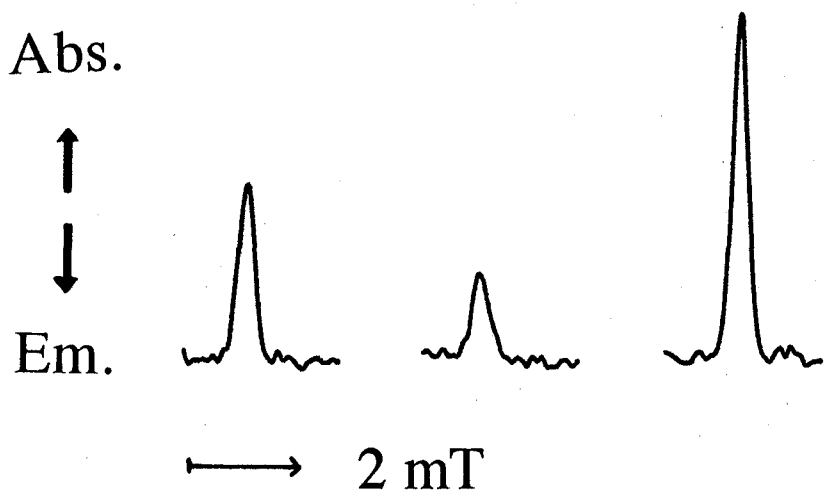

Figure (4.1) Time-resolved esr spectrum observed on the photolysis of TMDPO. Signal integration was carried out over the period between 200 ns and 400 ns after laser pulse.

equilibrium state by spectral pattern. The contribution of CIDEP must be evident in the observed signal, in order to discuss the reaction process of photofragmentation and the addition reaction of radicals. In the present studies, the CIDEP of the fragment radicals is examined on the photofragmentation of TMDPO by the time-resolved esr method.

The transient absorption studies have been carried out on the photolysis of other acylphosphine compounds.[8] The phospinoyl and thiophosphinoyl radicals have been detected. The time-resolved esr measurements, however, have not been carried out on the photolysis of TMTPO,TMDPS and TMTPS. In the present studies, the time-resolved esr measurements were carried out on the photolysis of these compounds.

4.2 Study on CIDEP in the photofragmentation of 2,4,6-trimethylbenzoylphosphine oxide (TMDPO) - effect of relaxation reagent -

The decay curves of esr signal are shown in Figure (4.2) for the high field peak of the diphenylphosphinoyl radical in the absence and the presence of $Cr(acac)_3$. In Figure (4.3) (a), the first-order decay constants k_{ap} are shown with the concentration of $Cr(acac)_3$. The decay was accelerated by the presence of $Cr(acac)_3$. The relaxation reagents such as $Cr(acac)_3$, which are chemically inert, can promote the spin-lattice relaxation by the spin exchange mechanism.[9] The accelerated decay of signal reflects the decay of CIDEP and this result is an evidence that the diphenylphosphinoyl radical shows the total-absorptive CIDEP. It is indicated that the CIDEP signal is much stronger than the

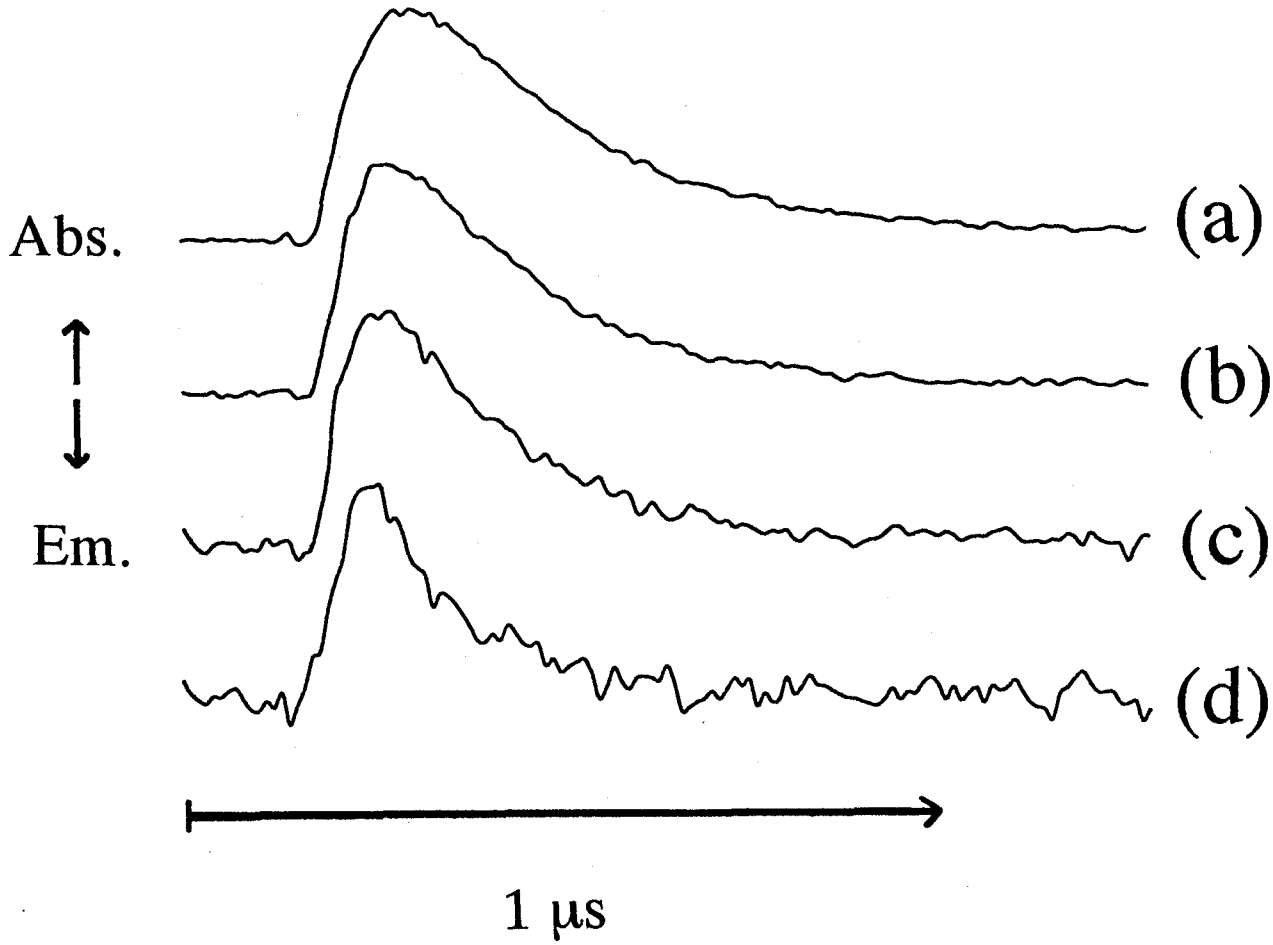

Figure (4.2) Time profiles of esr signal for the diphenylphosphinoyl radical at high field. The $Cr(acac)_3$ concentration is (a) 0, (b) 0.001, (c) 0.002, (d) 0.004 mol dm^{-3}.

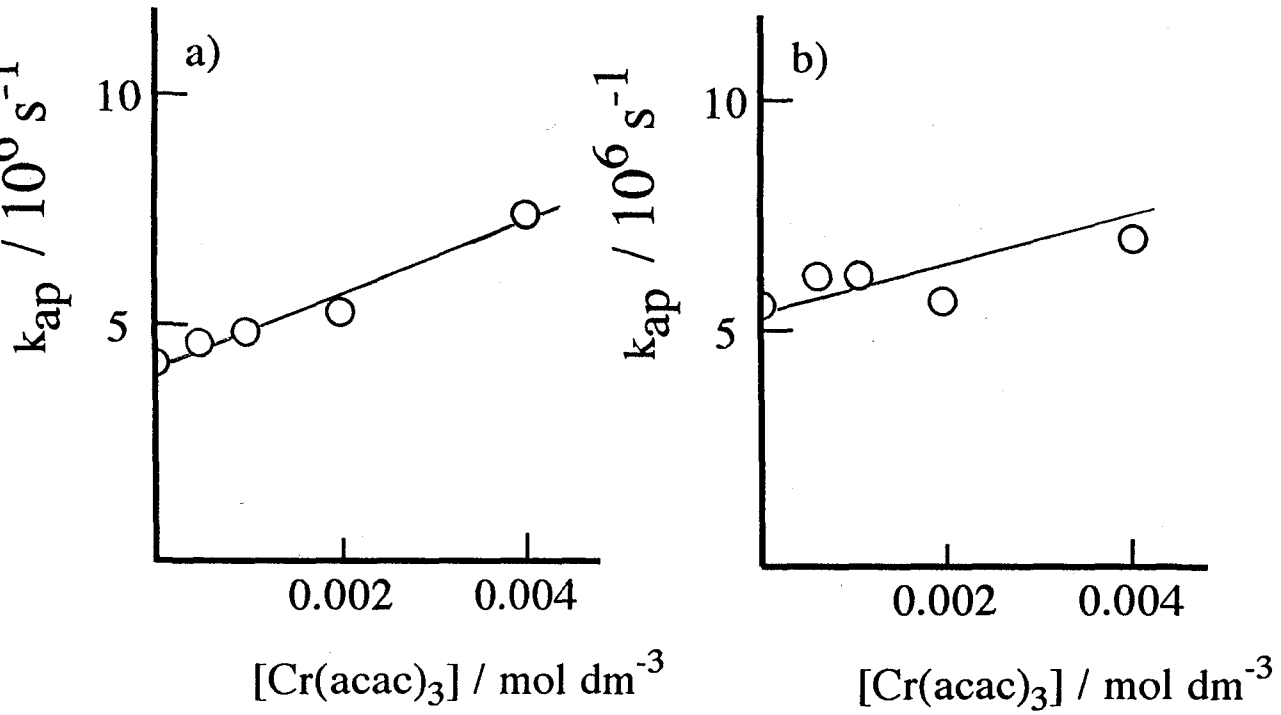

Figure (4.3) Dependence of the first-order decay constant k_{ap} on the $Cr(acac)_3$ concentration. a) the diphenylphosphinoyl radical at high field and b) the 2,4,6-trimethylbenzoyl radical.

thermal equilibrium one and the thermal equilibrium signal is negligible.

The first-order decay constants k_{ap} of the 2,4,6-trimethylbenzoyl radical are shown in Figure (4.3) (b). The decay was also accelerated by the presence of $Cr(acac)_3$. The 2,4,6-trimethylbenzoyl radical showed the absorptive CIDEP.

In the present system, the diphenylphosphinoyl radical and the 2,4,6-trimethylbenzoyl radical showed the absorptive CIDEP due to the TM. The radicals are formed from the excited triplet state of TMDPO. The E/A pattern of the diphenylphosphinoyl radical superposed on the total-absorptive signal agrees with the cleavage from the triplet state.

4.3 Study on CIDEP in the photofragmentation of TMDPO

- triplet quenching and polarization transfer -

The time-resolved esr measurements were carried out on the photolysis of TMDPO in the presence of naphthalene as a triplet quencher. In Figure (4.4), the ratio of signal intensities in the presence and the absence of naphthalene are shown as Stern-Volmer type plot for the diphenylphosphinoyl radical and the 2,4,6-trimethylbenzoyl radical. The signals, however, were not quenched. The triplet-triplet absorption of naphthalene is observed on the photolysis of TMDPO with naphthalene in the transient absorption experiment.[1)] The lowest triplet level of naphthalene is lower than that of TMDPO. Thus, the energy transfer can occur from the excited triplet state of TMDPO to naphthalene with respect to energy levels. The lifetime of the triplet excited state, however, is so short that naphthalene can not quench

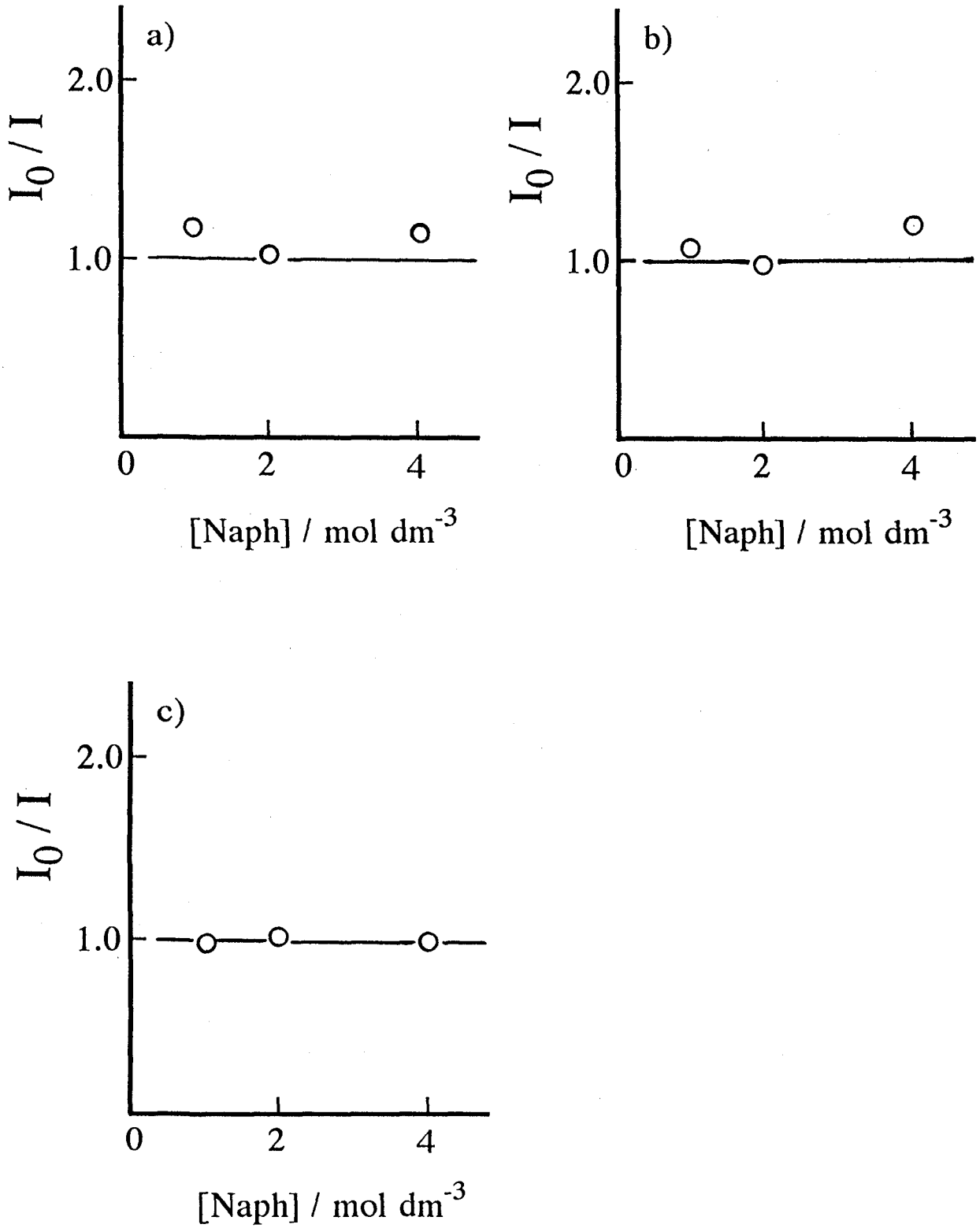

Figure (4.4) Stern-Volmer type plot for the ratio of esr intensities in the presence and absence of naphthalene. a) the diphenylphosphinoyl radical at high field, b) at low field, c) the 2,4,6- trimethylbenzoyl radical.

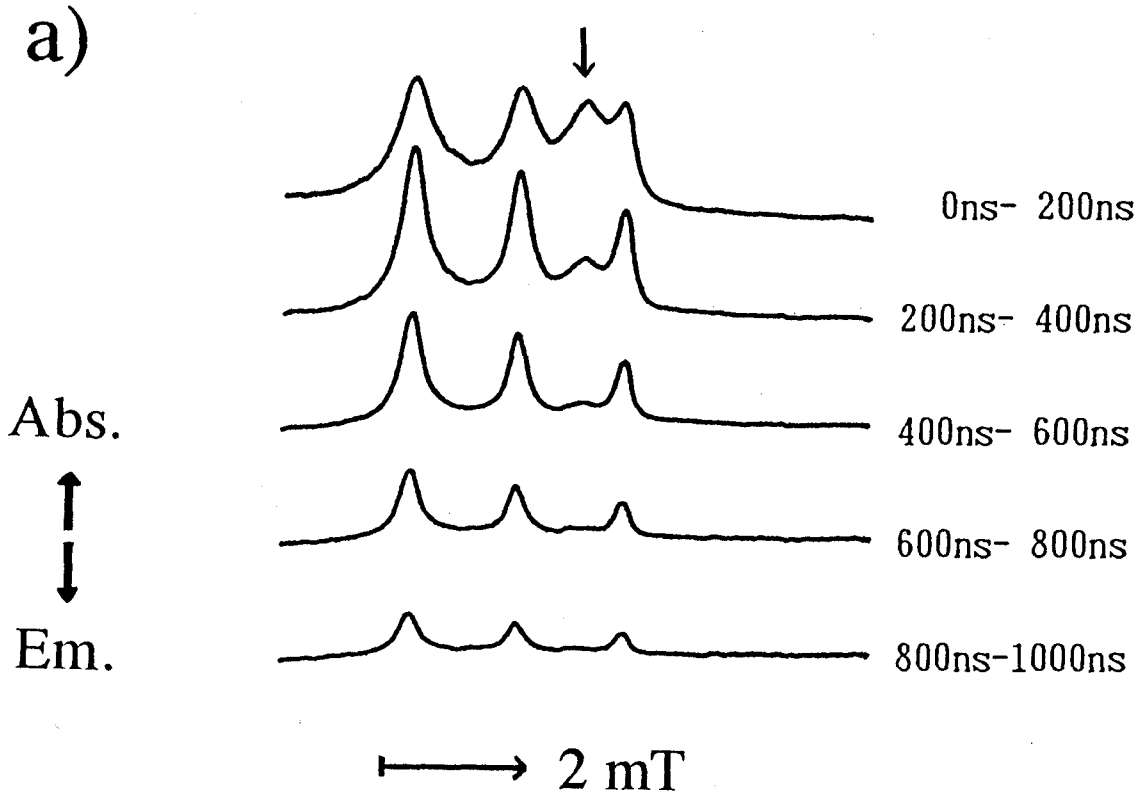

Figure (4.5) a) Time-resolved esr spectrum observed on the photolysis of TMDPO in the presence of ATEMPO (0.5 mol dm^{-3}). b) cw-esr spectrum of ATEMPO in benzene (0.01 mol dm^{-3}).

the esr signals. The fragmentation occurred before deactivation by quencher. Since the quenching did not occur in very high concentration of naphthalene (4 mol dm^{-3}), it was indicated that the lifetime was extremely short. In the transient absorption experiment, the same result has been reported and the lifetime has been estimated as 0.3 ns.[1] No oxygen effect to the esr signal was observed. The solved oxygen molecules can not quench the esr signal, because of the short lifetime of triplet state.

Time-resolved esr spectra observed on the photolysis of TMDPO in the presence of ATEMPO are shown in Figure (4.5). The spectra included two radical species, which showed different signal decays. One signal is due to the 2,4,6-trimethylbenzoyl radical formed by the photolysis of TMDPO. It is marked with an arrow in Figure (4.5). The other signal was assigned to the ATEMPO radical. A cw-esr spectrum of the ATEMPO radical (benzene solution of 0.01 mol dm^{-3}) is shown in Figure (4.5). The spectra of ATEMPO showed the total-absorptive CIDEP and decayed in the submicrosecond range. The different intensities of triplet lines are attributed to the decrease of samples in the cell. On the irradiation to ATEMPO without TMDPO, no CIDEP signal of ATEMPO was observed. The origin of the CIDEP is concerned with the photolysis of TMDPO. Three possible interpretations exist for the observed CIDEP. They are (1) triplet-doublet polarization transfer, (2) spin polarization generation in the triplet-doublet interaction and (3) doublet-doublet polarization transfer.[10-12] In the case of triplet-doublet polarization transfer, the spin polarization would transfer to ATEMPO from the triplet-excited state of TMDPO, which would possess absorptive polarization. In

the case of polarization generation, the interaction between the triplet excited state of TMDPO and the ATEMPO doublet would generate CIDEP which shows emission.[11] The observed signal, however, showed the absorptive CIDEP. Thus, the polarization generation of the triplet-doublet interaction can be excluded. In the case of doublet-doublet polarization transfer, the spin polarization would transfer to ATEMPO from the doublet radicals formed by the photolysis of TMDPO. The doublet-doublet polarization transfer results from the spin exchange of radicals.

The lifetime of triplet excited state needs to be sufficiently long for the triplet-doulet polarization transfer and the polarization generation of the triplet-doublet interaction. Neither the triplet-doublet polarization transfer nor generation can occur in the present TMDPO/ATEMPO system, because the lifetime of triplet state is very short. In the ATEMPO concentration of 0.05 mol dm^{-3}, the fragmentation of TMDPO would be much faster than the collision with ATEMPO. Then, it is concluded that the observed CIDEP of ATEMPO results from the doublet-doublet polarization transfer. In the presence of ATEMPO, the signal of the diphenylphosphinoyl radical was extremely weak and the decay was accelerated. Although the chemical reaction with ATEMPO can also affect the signal, this quenching would support the spin exchange between ATEMPO and the diphenylphosphinoyl radical. This result is another evidence that the fragment radicals of TMDPO possess the total-absorptive CIDEP due to the TM.

In the Scheme (4.1), the photolysis of TMDPO is shown for the present system. In the case of total-absorptive esr signal

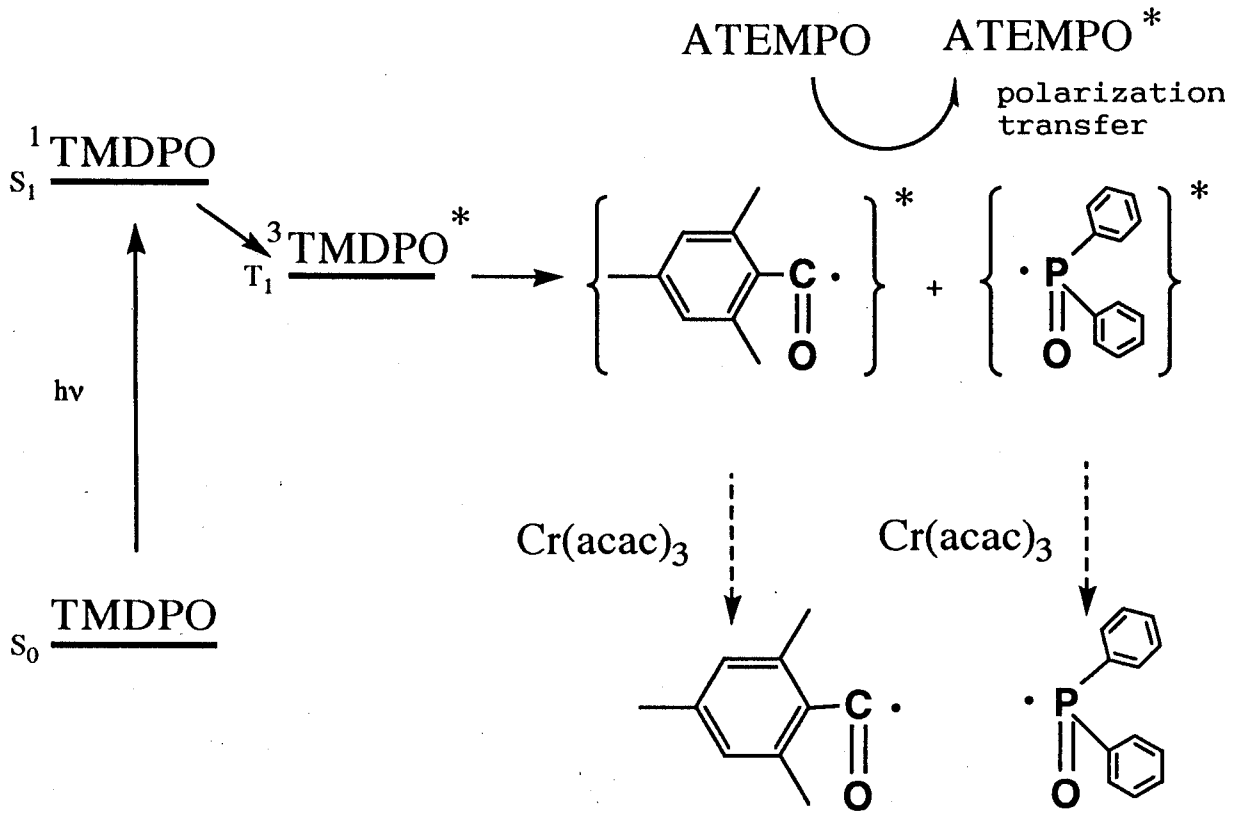

Scheme (4.1) Total-absorptive CIDEP in the photolysis of TMDPO. The asterisk denotes the total-absorptive CIDEP due to the TM in the present scheme.

which can be the thermal equilibrium one, the effect of relaxation reagent, the triplet quenching and the polarization transfer are useful for examination of CIDEP.

4.4 Time-resolved esr studies on photofragmentation of other derivatives

A time-resolved esr spectrum observed on the photolysis of TMTPO is shown in Figure (4.6). It was identical with that of TMDPO. Three absorptive esr lines exist in the spectrum. The two resonance peaks at the highest and the lowest magnetic field are due to the phosphinoyl radical, which exhibits the hfs by a phosphorus nucleus. This signal is due to the di-*o*-tolylphosphinoyl radical in the present case. The hfc of the phosphorus nucleus was 36.1 mT. A weak E/A pattern due to the RPM was superposed on a total-absorptive signal. The central peak is due to the 2,4,6-trimethylbenzoyl radical with no hfs. The reactivity of the di-*o*-tolylphosphinoyl radical is described in chapter 5.

On the photolysis of TMDPS in benzene, the time-resolved esr spectrum shown in Figure (4.7) (a) was observed. The spectrum consists of two esr lines. The high field line was absorptive and the low field line was emissive respectively. The spectrum was assigned to the diphenylthiophosphinoyl radical, which showed the E^*/A pattern of esr signal. (The asterisk * denotes more intense line.) The hfc of a phosphorus nucleus was 29.0 mT and the g-value was 2.008.[13] The esr signal of the counter radical which was the 2,4,6-trimethylbenzoyl radical, however, was not observed.

On the photolysis of TMTPS in benzene, the time-resolved esr

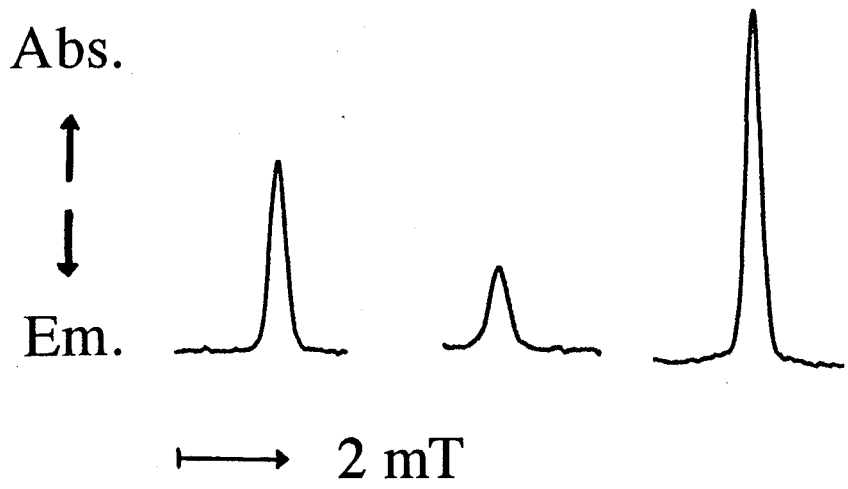

Figure (4.6) Time-resolved esr spectrum observed on the photolysis of TMTPO. Signal integration was carried out over the period between 200 ns and 400 ns after laser pulse.

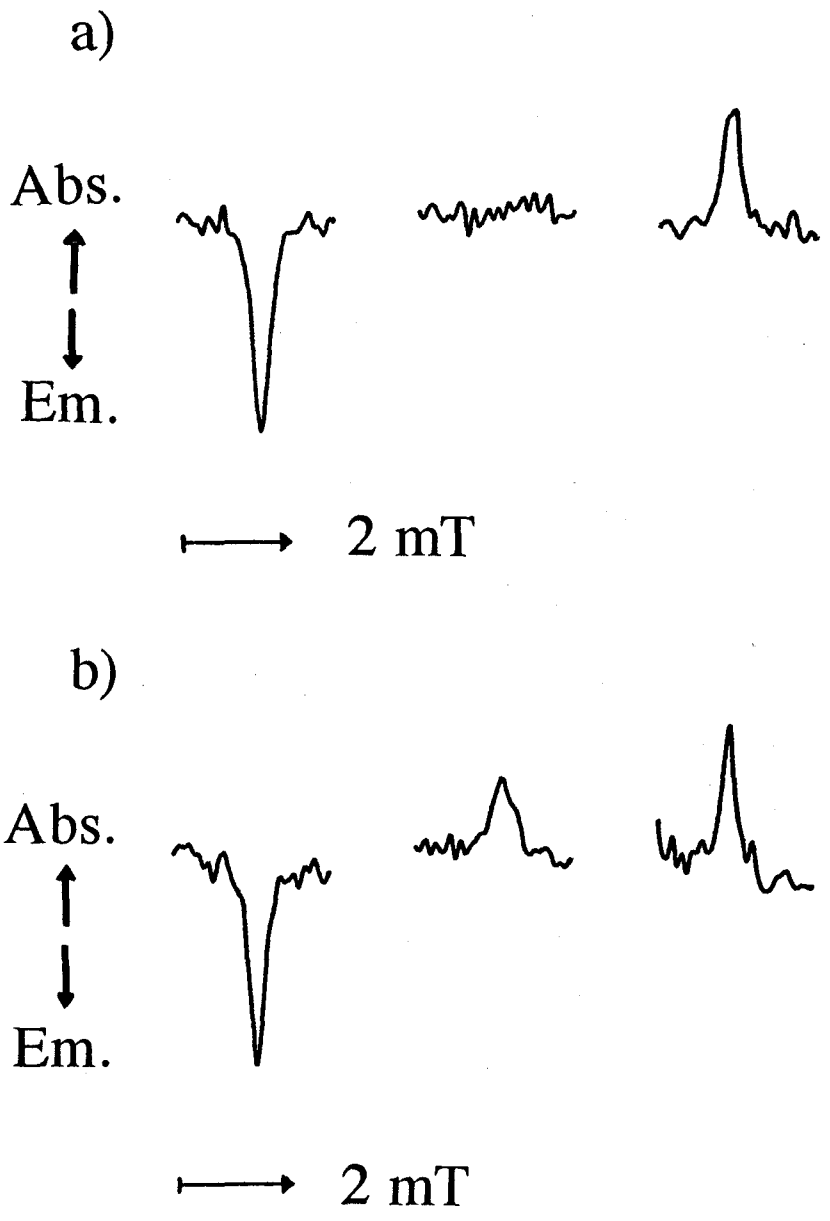

Figure (4.7) Time-resolved esr spectra observed on the photolysis of a) TMDPS and b) TMTPS. Signal integration was carried out over the period between 200 ns and 400 ns after laser pulse.

spectrum shown in Figure (4.7) (b) was observed. In the case of TMTPS, the spectrum consists of three esr lines. The high field line and the central line were absorptive and the low field line was emissive respectively. The high field and the low field lines are due to the di-o-tolylthiophosphinoyl radical, which showed the E^*/A pattern of esr signal. The hfc of a phosphorus nucleus was 29.0 mT and the g-value was 2.009.[13] The central line at 2.001 of the g-value is due to the 2,4,6-trimethylbenzoyl radical, the counter radical.

The diphenylthiophosphinoyl radical and the di-o-tolylthiophosphinoyl radical showed almost the identical spectrum. The substitution of aromatic protons at the ortho position by the methyl groups did not affect the time-resolved esr spectra of the thiophosphinoyl radicals as well as the phosphinoyl radicals. The esr signal of the counter radical, however, was affected by the substitution in the thiophosphinoyl radicals. On the photolysis of TMDPS, the esr signal of the 2,4,6-trimethylbenzoyl radical disappeared, while that from TMTPS was observed. The disappearance of the esr signal is reported for the substitution of methyl groups at the ortho position by the methoxy groups in the 2,4,6-trimethylbenzoyl radical itself.[14] In the present case, however, the substitution affected only the esr signal of the counter radical.

No contribution of a total-absorptive signal exists in the spectra of the thiophosphinoyl radicals in comparison with that of the phosphinoyl radicals. The total-absorptive CIDEP due to the TM may be disappeared on the photolysis of acylphosphine sulphides. The observed signals of the thiophosphinoyl radicals

were not as intense as those of the phosphinoyl radicals. The fast relaxation of the triplet sublevels in the triplet exited state or the long lifetime of the triplet precursor can remove the CIDEP due to the TM from radicals, because the spin polarization disappears by the relaxation before the chemical reaction.[15] The E^*/A pattern of the spectra is due to the T-precursor RPM of ST_0mixing and an emissive distortion. The photolysis occurs in the triplet excited state.

The origin of distortion would be the RPM of ST_mixing.[16] The ST_mixing CIDEP shows the emissive signal in the case of T-precursor pair. In radicals of large hfc, such as the phosphinoyl radicals, the ST_mixing occurs easily, because the hyperfine interaction causes the ST_mixing. The CIDEP due to the ST_mixing is reported for the radicals of large hfc, including the phosphorus-centered radicals.[16c,16d,16e] The polarization due to the ST_mixing is represented as

$$P(ST\_) = \pi A^2 r_c/(4g\mu_B H\lambda D), \qquad (4.1)$$

in the asymptotic region by the stochastic Liouville method.[16a,16b] In the equation (4.1), A is the hfc, r_c is the separation of the level crossing, H is the magnetic field, λ is the exponent factor in the exponential exchange interaction, D is the diffusion constant of the radical pair and the others have their usual meanings. The polarization is proportional to the square of A.

In Figure (4.8), time-resolved esr spectra are shown on the

photolysis of TMTPS in *n*-dodecane and *n*-hexane. The viscosity η of *n*-dodecane is 1.466 mPa s, that of benzene is 0.652 mPa s and that of *n*-hexane is 0.310 mPa s respectively. The intensity ratio of high field and low field line, (I_h/I_l), shows the contribution of emissive distortion.[16e] A small value of (I_h/I_l) indicates large contribution of distortion. The ratio (I_h/I_l) decreased as the viscosity of solvent increased, (0.87) in *n*-hexane, (0.70) in benzene, and (0.23) in *n*-dodecane. This result supported the ST_mixing CIDEP. As shown in equation (4.1), the ST_mixing is dependent on the diffusion constant D. The radical pair can remain for long time in the level crossing region by slow diffusion. Then, the slow diffusion, that is, the high viscosity enhances the contribution of the ST_mixing CIDEP. The polarization due to the ST_mixing is proportional to η, by the relation of $D = kT/(4\pi a\eta)$, where a is the molecular radius of solvent. On the other hand, the polarization due to the TM is independent of the diffusion constant. Thus, the emissive distortion of spectra can not be attributed to the emissive CIDEP due to the TM. The polarization due to the ST_0mixing in the different g-values causes the distortion. In this case, however, the ratio (I_h/I_l) is also independent of the diffusion constant. Then, the viscosity dependence of the distortion would be attributed to the ST_mixing CIDEP.

The signal of the 2,4,6-trimethylbenzoyl radical was absorptive on the photolysis of TMTPS. The difference of g-values can cause the polarization due to the ST_0mixing. In the radical pair with the thiophosphinoyl radical, the 2,4,6-trimethylbenzoyl radical can show an absorptive CIDEP. Thus, this signal can be

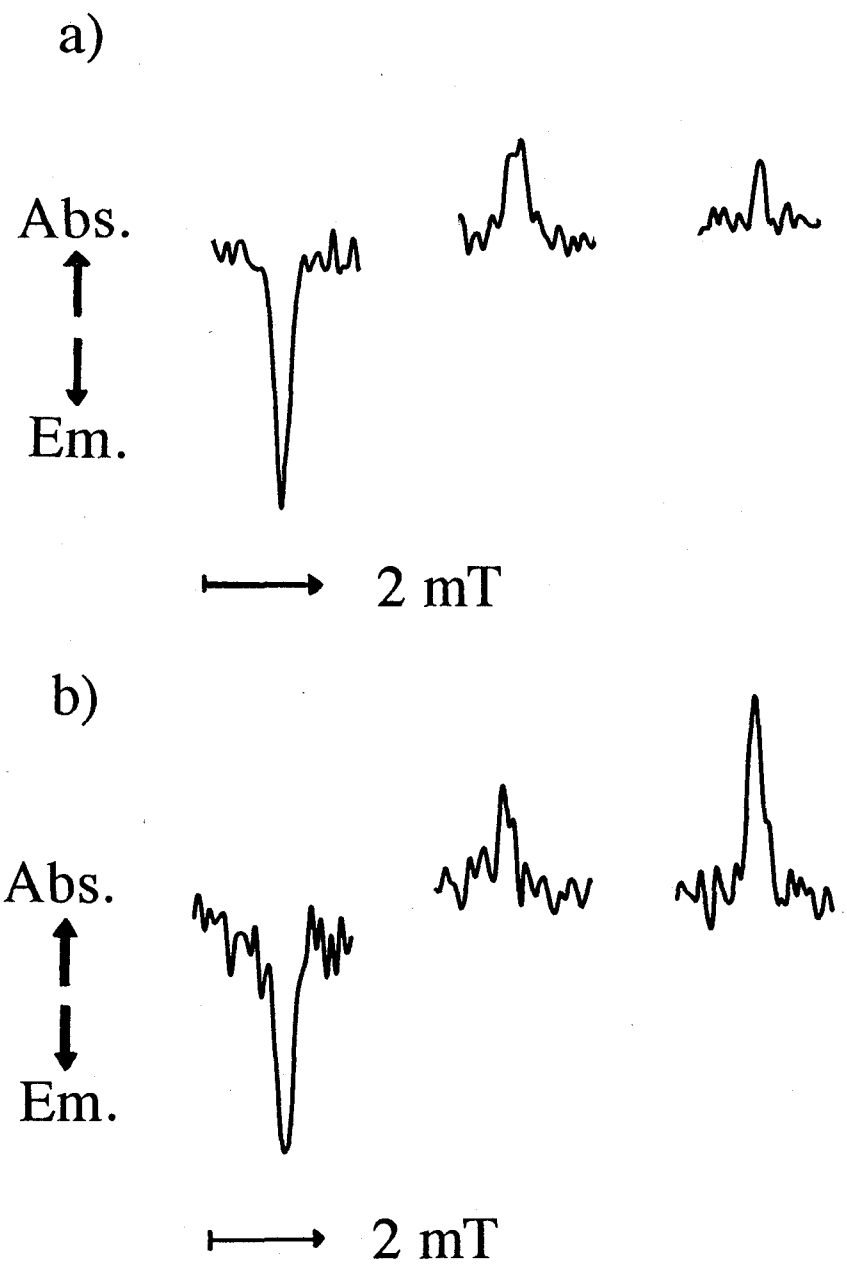

Figure (4.8) Time-resolved esr spectra observed on the photolysis of TMTPS in a) *n*-dodecane and b) *n*-hexane. Signal integration was carried out over the period between 200 ns and 400 ns after laser pulse.

due to the ST_0mixing. As shown in Figure (4.8), no dependence appears to exist on the viscosity of solvent. The contribution of ST_mixing, which was emissive, was not observed for the 2,4,6-trimethylbenzoyl radical. The details of CIDEP, however, are unknown for the 2,4,6-trimethylbenzoyl radical.

The time-resolved esr signals of the thiophosphinoyl radicals are observed. The initiation reaction, however, can not observed by the time-resolved esr method, because the total-absorptive polarization which is very intense is absent. The signal intensity is too small to observe the reaction process of radical. It would be difficult to observe the product radical by the polarization transfer in the reaction of thiophosphinpyl radical.

4.5 Discussion on esr signal decays

The esr signal of the diphenylphosphinoyl radical shows the single exponential decay. The decay rate is independent of the microwave power and affected by chemical reactions as described in chapter 5. As demonstrated in chapter 3., three possible cases exist that can reproduce the observed exponential decay which is independent of microwave power in the presence of first-order chemical reactions. It is the first case that the observed signal is at the thermal equilibrium in the initial state. In the present study, however, the evidences of CIDEP were obtained. Thus, the thermal equilibrium case is excluded. The second is the fast reaction case. In this case, the signal decay is due to fast chemical reactions only, as represented by equation (3.6). On the other hand, it is the third case that the thermal equilibrium

signal is negligible and the CIDEP signal decay is due to both reactions and relaxation, as represented by equation (3.7). By the experiment of relaxation reagent, it is found that the contribution of thermal equilibrium signal is negligible, that is, $m_0 >> P_{eq}n_0/(1 + T_1T_2\omega_1^2)$. Then, one condition of the third case is satisfied in the present system. In the presence of relaxation reagent, the signal decay reflected the decay of CIDEP. In the absence of relaxation reagent, however, the contribution of relaxation to the decay of signal can not be observed from the present experiments. The second and the third case are possible in the present system. In order to determine whether the second or the third case, the spin-lattice relaxation time T_1 needs to be observed directly.

References to chapter 4

1. T.Sumiyoshi and W.Schnabel, Polymer, 26, 141(1985).
2. J.E.Baxter, R.S.Davidson, H.J.Hageman and T.Overeem, Makromol. Chem., Rapid. Commun., 8 311(1987).
3. J.E.Baxter, R.S.Davidson, H.J.Hageman and T.Overeem, Makromol. Chem. 189, 2769(1988).
4. Y.Yagci, J.Borebely and W.Schnabel, Eur. Polym. J. 25, 129(1988).
5. T.Sumiyoshi, A.Henne, P.Lechtken and W.Schnabel, Z. Naturforsch., A39,434(1984).
6. J.E.Baxter, R.S.Davidson, H.J.Hegeman, K.A.McLauchlan and D.G.Steven, J. Cem. Soc. Commun., 2, 73(1987).
7. M.Kamachi, K.Kuwata, T.Sumiyoshi and W.Schnabel, J. Chem. Soc. Perkin Trans 2, 961(1988).
8. (a) T.Sumiyoshi, W.Weber and W.Schnabel, Z.Naturforsch, Teil A, 40, 541(1985).
   (b) T.Majima and W.Schnabel, J. Photochem. Photobiol., A, 50, 31(1989).
9. (a) O. A. Gansow, K. G. R. Pachler and G. N. LaMar, J. Chem. Soc., Chem. Commun., 456(1972).
   (b) Y. Sakaguchi and H. Hayashi, Chem. Phys. Lett., 106, 420(1984).
   (c) N. J. Turro, X. Lei, I. R. Gould and M.B. Zimmt, Chem. Phys. Lett., 120, 397(1985).
   (d) Y. Tanimoto, A.Kita, M. Itoh, M. Okazaki, R. Nakagaki and S. Nagakura, Chem. Phys. Lett., 165, 184(1990).
   (e) J. S. Hyde and T. Sarna, J. Chem. Phys., 68, 4439(1978).
10. (a) T. Imamura, O. Onitsuka and K. Obi, J. Phys. Chem., 90,

6741(1986).

(b) T. Okutsu, A. Kawai and K. Obi, J. Phys. Chem., 93, 7757(1989).

11. (a) C. Blattler, F. Jent and H.Paul, Chem. Phys. Lett., 166, 375(1988).

(b) A. Kawai, T. Okutsu and K. Obi, J. Phys. Chem., 95, 9130(1991).

12. W. S. Jenks and N. J. Turro, J. Am. Chem. Soc., 112, 9009(1990).

13. R.A.J.Janssen, M.H.W.Sonnemans and H.M.Buck, J. Chem. Phys., 84, 3694(1986).

14. T.Majima, Y.Konishi, A.Bottecher, K.Kuwata, M.Kamachi and W.Schnabel, J. Photochem. Photobiol., A, 58, 239(1991).

15. (a) J.K.S.Wan, S.Wong and D.A.Hutchison, Acc. Chem. Res.,7, 58(1974).

(b) J.K.S.Wan and A.J.Elliot, Acc. Chem. Res., 10, 161(1977).

(c) P. J. Hore, C. G. Joslin and K. A. McLauchlan, Chem. Soc. Rev., 8, 29(1979).

(d) C. D. Backley and K. A. McLauchlan, Mol. Phys., 54, 1(1985).

(e) K.A.McLauchlan and D.G.Stevens, Acc. Chem. Res., 21, 54(1988).

(f) J.H.Freed and J.B.Pedersen, Adv. Mag. Resonance, 8, 2(1976), Academic Press.

(g) L.Kevan and R.N.Schwartz(editor), Time Domain Electron Spin Resonance, Wiley-Interscience (1979).

16. (a) F.J.Adrian and L.Monchick, J. Chem. Phys., 71, 2600(1979).

(b) F.J.Adrian and L.Monchick, J. Chem. Phys., 72, 5796(1980).

(c) T.J.Burkey, J.Lusztyk, K.U.Ingold, J.K.S.Wan and F.J.Adrian, J. Phys. Chem., 89, 4286(1985).

(d) C.D.Buckley and K.A.McLauchlan, Chem. Phys. Lett., 137, 86(1987).

(e) F.J.Adrian, K.Akiyama, K.U.Ingold and J.K.S.Wan, Chem. Phys. Lett., 155, 333(1988).

5. Initiation step in photopolymerization

5.1 Initiation reaction by the photofragment radicals of acylphosphine compounds

The addition reaction of the diphenylphosphinoyl radical has been studied with several monomers by the transient absorption method.[1] The rate constants are determined from the decay of the radical. They are in the range of 10^6 - 10^7 mol dm^{-3}. The diphenylphosphinoyl radical is found to be very reactive to vinyl monomers. The di-*o*-tolylphosphinoyl radical has also been studied for the addition reaction by the transient absorption method.[2] The rate constants of di-*o*-tolylphosphinoyl radical are about ten times as small as that of the diphenylphosphinoyl radical. The di-*o*-tolylphosphinoyl radical is less reactive to vinyl monomers than the diphenylphosphinoyl radical, because of the substitution effect in the ortho positions of phenyl groups. In the present studies, the addition reaction of these phosphinoyl radicals, that is, the initiation reaction was observed directly by the time-resolved esr method.

The products of addition reaction are detected on the photofragmentation of TMDPO in the presence of vinyl monomers by the product analysis method.[3] The initiation efficiency of the diphenylphosphinoyl radical is twice that of the 2,4,6-trimethylbenzoyl radical. It is indicated that the diphenylphosphinoyl radical is more reactive to vinyl monomers than the 2,4,6-trimethylbenzoyl radical. Furthermore, the 2,4,6-trimethylbenzoyl radical is more susceptible to oxygen, according to the result of product analysis. In the present studies, the reactivity was examined for these fragment radicals by the time-resolved esr

method.

The thiophosphinoyl radicals formed in the photofragmentation of TMDPS and TMTPS have been studied on the addition reaction by the transient absorption method.[2,4] The reactivity is lower than that of the diphenylphosphinoyl radical. The rate constants are reported to be about one order of magnitude lower than those of the diphenylphosphinoyl radical. The time-resolved esr observation, however, is difficult on the initiation reaction of the thiophosphinoyl radicals, because the intense total-absorptive CIDEP due to the TM is absent, as described in Chapter 4.

5.2 Observation of the primary propagating radical

A time-resolved esr spectrum shown in Figure (5.1) was obtained by the time integration of signal over the period between 200 ns and 400 ns after laser irradiation on the photolysis of TMDPO with αMS, where the αMS concentration was 0.5 mol dm^{-3}. By computer simulation, the spectrum was assigned to the product radical formed by the addition of the olefinic compound to the diphenylphosphinoyl radical, αMS. This addition reaction yields radical (I) as a product radical, as shown in Scheme (5.1). The simulated spectrum of radical (I) is shown in Figure (5.1). (The central peak is due to the 2,4,6-trimethylbenzoyl radical.) In the simulation, the modified parameters from similar radicals were used.[5] The hfc of the phosphorus nucleus was estimated to be 5.3 mT by comparison of the simulated spectrum with the observed one. The esr spectrum of radical (I) can be discriminat-

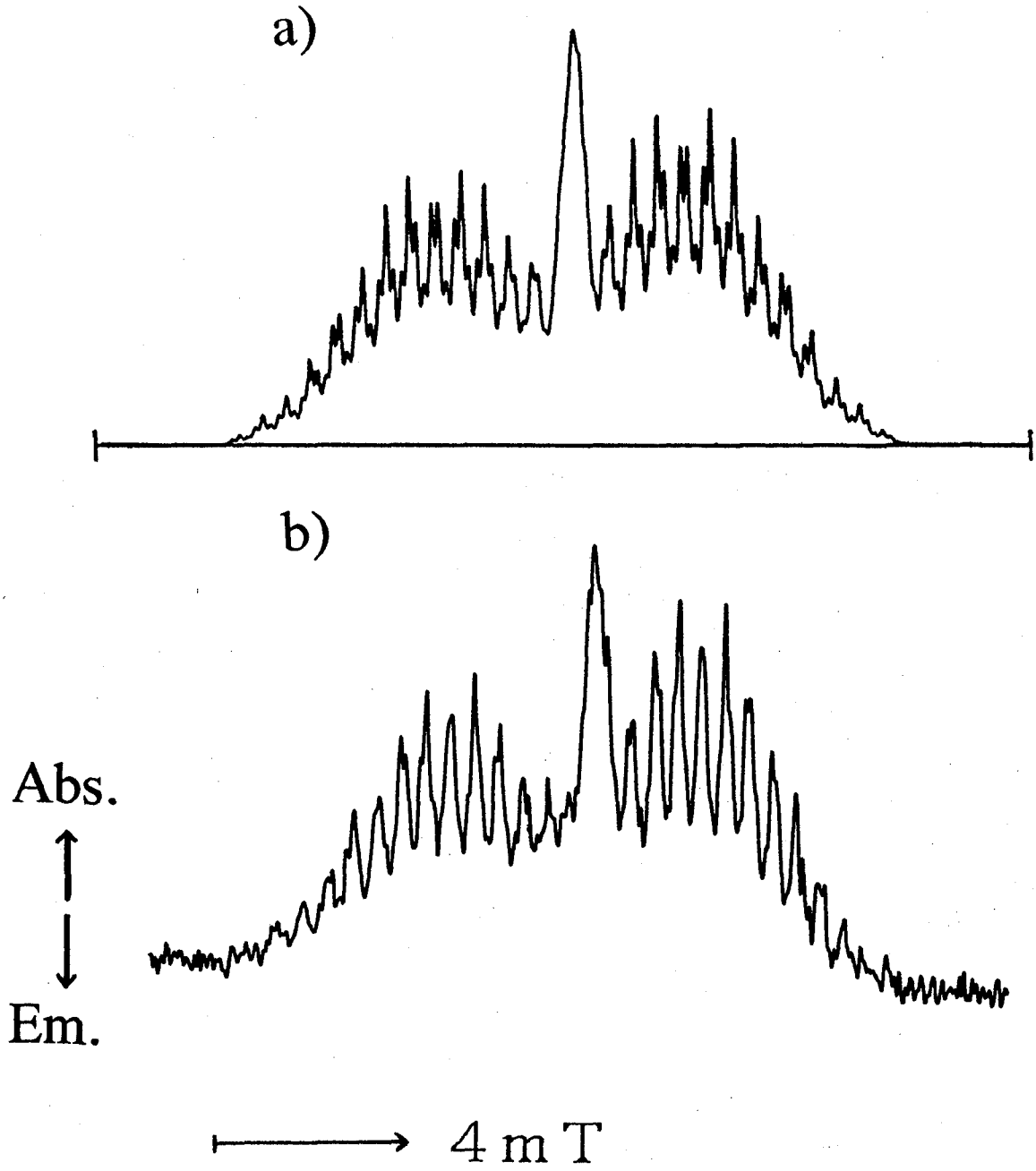

Figure (5.1) a) Computer simulation of esr spectrum for the radical formed by the addition of the diphenylphosphinoyl radical to αMS. b) Time-resolved esr spectrum observed on the photolysis of TMDPO in the presence of αMS (0.5 mol dm^{-3}). Signal integration was carried out over the period between 200 ns and 400 ns after laser pulse.

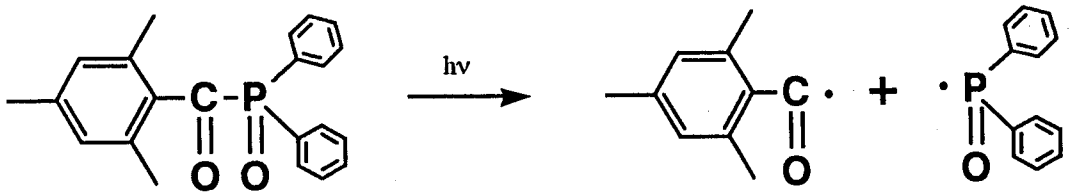

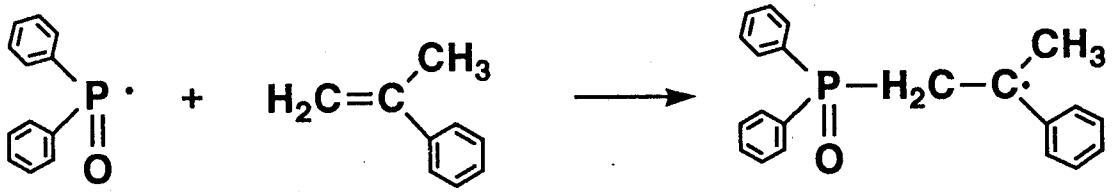

radical (I)

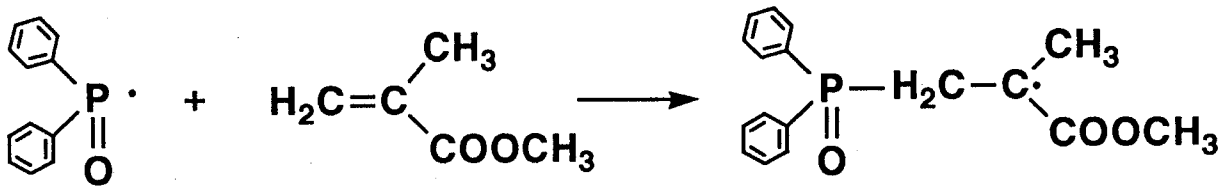

radical (II)

Scheme (5.1) Addition reactions of the diphenylphosphinoyl radical to αMS and MMA.

ed from that of the product radical formed by the addition to a carbon-centered radical, such as the 2,4,6-trimethylbenzoyl radical, because of the hfs due to the phosphorus nucleus. The esr signal of the diphenylphosphinoyl radical was quenched at the αMS concentration of 0.5 mol dm^{-3}. This result also indicates the reaction of the diphenylphosphinoyl radical.

The signal decay of radical (I) depended on the microwave power of esr spectrometer, as demonstrated in Figure (5.2). At the high microwave power level, the decay curves showed nutation. This result indicates that the decay was not due to chemical reactions but the spin-lattice relaxation of spin polarization induced by microwave absorption. The lifetime of radical (I) is much longer than the decay of esr signal. Thus, the esr signal of the product radical is due to CIDEP. As shown in the spectrum, radical (I) showed a total-absorptive spin polarization. This spin polarization is attributed to the polarization transfer[6] in the addition reaction, from the diphenylphosphinoyl radical to the product radical. As demonstrated in chapter 4., the diphenylphosphinoyl radical showed the total-absorptive CIDEP. This polarization transfer is also an evidence that the signal of the diphenylphosphinoyl radical is due to the total-absorptive CIDEP. The product radical can be observed due to the polarization transfer.

A product radical was also detected in the photolysis of TMDPO with MMA, where the MMA concentration was 0.5 mol dm^{-3}. The time-resolved esr spectrum of the product radical and a simulated spectrum of the product radical are shown in Figure (5.3). The spectrum was identified as radical (II) by computer simulation

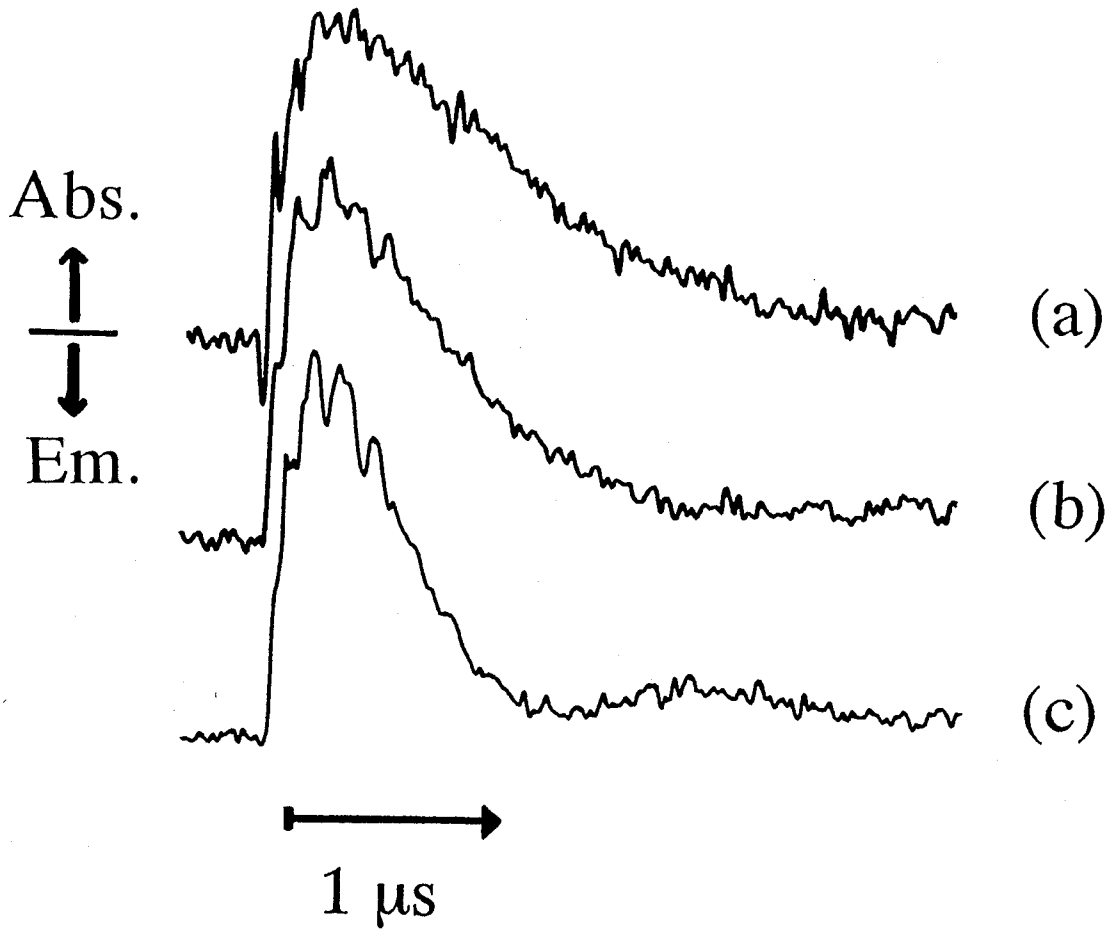

Figure (5.2) Time profiles of esr signal for the product radical at the αMS concentration of 0.5 mol dm^{-3}. Microwave power is (a) 17 dB, (b) 14 dB, (c) 10 dB.

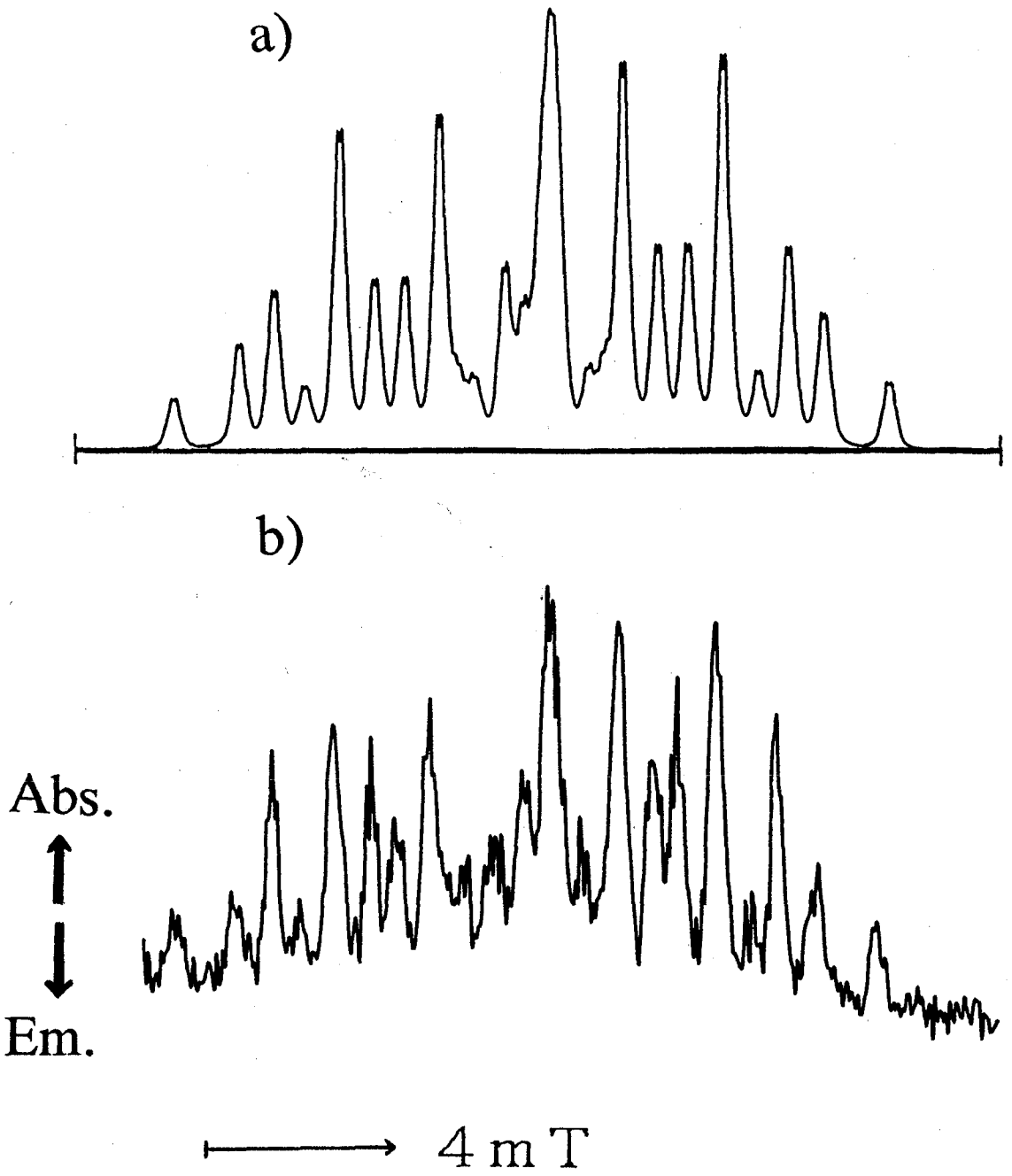

Figure (5.3) a) Computer simulation of esr spectrum for the radical formed by the addition of the diphenylphosphinoyl radical to MMA. b) Time-resolved esr spectrum observed on the photolysis of TMDPO in the presence of MMA (0.5 mol dm^{-3}). Signal integration was carried out over the period between 200 ns and 400 ns after laser pulse.

using the modified parameters from those of similar radicals.[7] The hfc of the phosphorus nucleus was estimated to be 6.1 mT. The diphenylphosphinoyl radical also reacted with MMA, as shown in Scheme (5.1).

This addition reaction is an initiation process of polymerization. *The primary propagating radical* of MMA, that is, radical (II) was formed by addition of a monomer molecule to a fragment radical of initiator. The propagation of polymer molecule follows *the initiation step*. The spectrum of the primary propagating radical of monomer can be discriminated from the secondary propagating radical and the higher propagating radicals, because of the hfs due to the phosphorus nucleus. In the present study, the initiation process in polymerization of MMA was directly observed by the time-resoled esr spectroscopy.

The secondary and higher propagating radicals in propagation process were not observed in the present system. The rate constant of propagation of MMA has been reported as ~ 10^2 s^{-1} mol^{-1} dm^3 in general. The propagation reaction is much slower than the initiation reaction of the diphenylphosphinoyl radical with MMA. Then, the primary propagating radical does not react with another MMA molecule in the observed time region. The spin polarization relaxes before the reaction, so that the secondary or higher propagating radicals can not be detected by the time-resolved measurement.

In the steady-state esr experiments, the detections of propagating radicals have been reported in photopolymerization of MMA with azocompounds.[8] According to the discussion, however, the observed radicals are the polymerized ones including several

monomer units. No primary propagating radical was detected in the steady-state polymerization.

The primary propagating radical of monomer can be observed by the time-resolved esr method. In the present system, the polarization transfer enables to observe the primary propagating radical. The higher propagating radicals are not observed due to the decay of CIDEP, so that the primary propagating radical can be observed by itself. On the other hand, the primary propagating radical is not observed in the stady-state experiment, because of the low concentration. By the stady-state esr method, the terminal radicals of polymer chain were studied. The time-resolved esr and the stady-state esr method can be useful to different steps in radical polymerization respectively.

5.3 Determination of rate constants from esr signal decays

The time-resolved esr signal of the diphenylphosphinoyl radical was affected by the presence of αMS. The signal intensity decreased as the αMS concentration increased. The time profile of esr signal was also affected by the presence of αMS. As the concentration of αMS increased, the decay was accelerated. The accelerated decay curve with αMS also followed the first-order kinetics as shown in Figure (5.4). The apparent first-order decay constants k_{ap} were obtained at some concentrations of αMS. As shown in Figure (5.5), k_{ap} increased with the concentration of αMS and their linear relationship can be represented by

$$k_{ap} = k[\alpha MS] + k_0, \qquad (5.1)$$

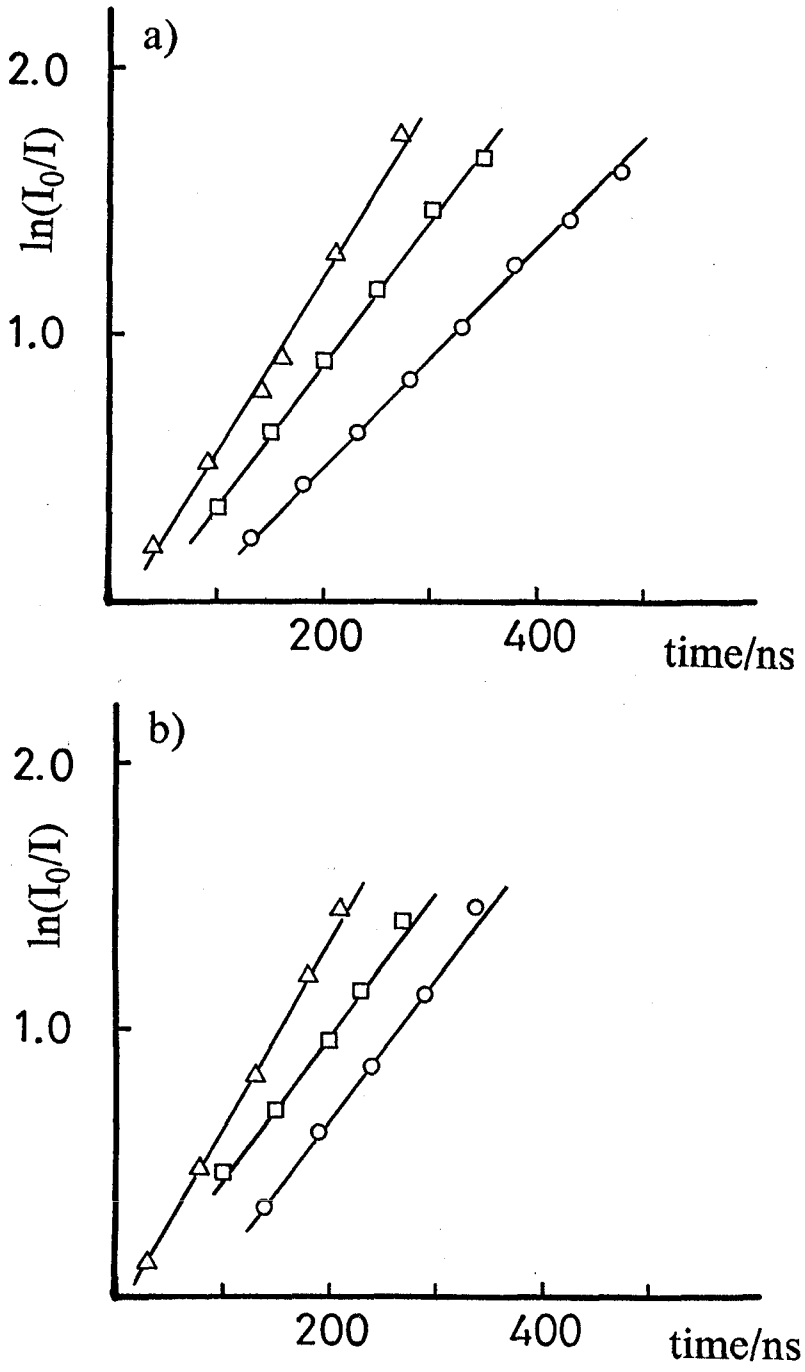

Figure (5.4) First-order decays of the diphenylphosphinoyl radical at a) high field and b) low field. ○: neat, □: at the αMS concentration of 0.1 mol dm^{-3}, △: 0.2 mol dm^{-3}.

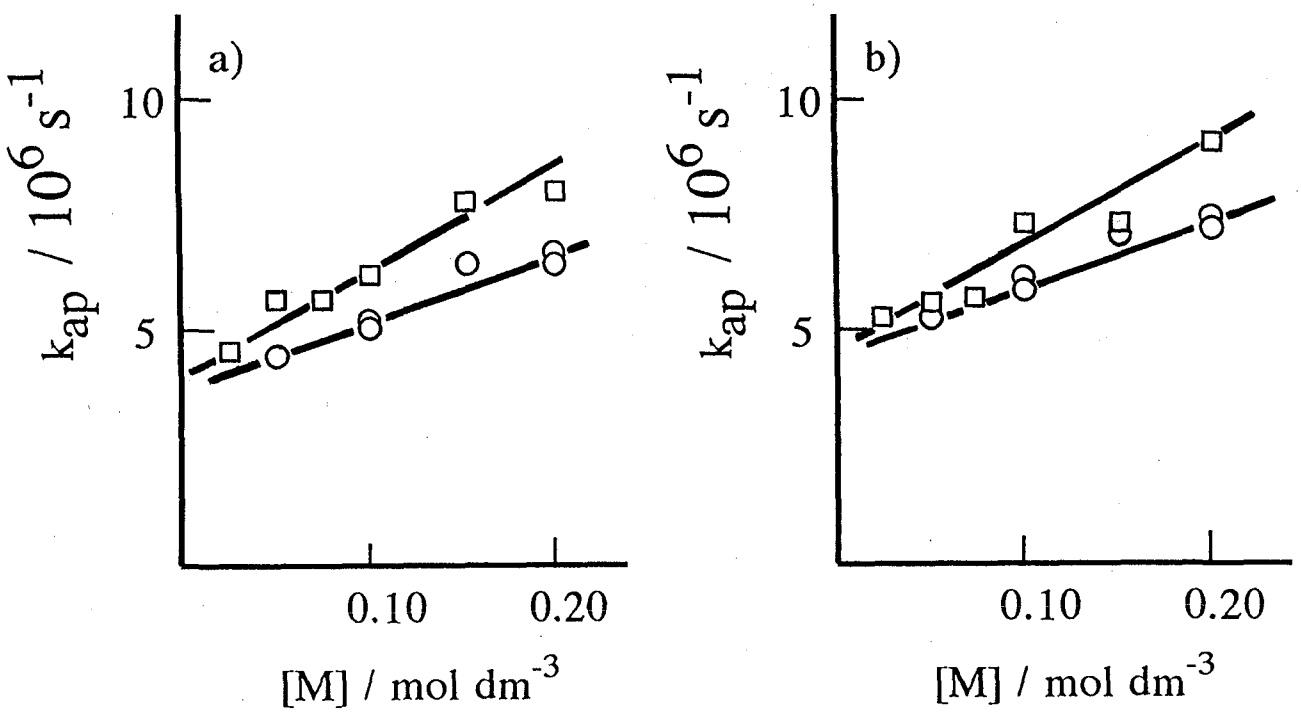

Figure (5.5) Dependence of the first-order decay constant k_{ap} of the diphenylphosphinoyl radical on the monomer concentration at a) high field and b) low field. ○: αMS, □: MMA.

where [αMS] denotes the concentration of αMS. The intercept k_0 is the apparent first-order decay constant in the absence of αMS. The term k[αMS] is a pseudo-first-order rate constant of the diphenylphosphinoyl radical, where k is the second-order rate constant of addition of αMS. The value of k was obtained at the high field peak and the low field peak, respectively. These values were in agreement to each other within the error of the present experiment. The value of k was obtained to be (1.5 ±0.2) 10^7 mol^{-1} dm^3 s^{-1} for αMS.

The generation of spin polarization due to the F-pair distorts the decay curve of esr signal. The spin polarization due to the F-pair shows the E/A pattern. In the present case, the high field peak showed absorptive signal and the low field peak showed emissive signal in the later stage of decay.[9] Thus, to a small extent, the high field decay was distorted absorptively and the low field decay was distorted emissively. This distortion would cause the difference between k_{ap} of the high field peak and that of the low field peak. The value of k_{ap} at the low field peak is larger than that of the high field peak as shown in Figure (5.5). Thus, the agreement of the value of k suggests that the value of k is not affected by the CIDEP due to the F-pair mechanism. The distortion of decay curve may be included in the k_0 term. The k_0 term would reflect the other reactions, such as the reaction with TMDPO, and the contribution of the spin-lattice relaxation.[9]

On the diphenylphosphinoyl radical, the behaviors of esr signal with MMA were similar to that with αMS. The accelerated

decay curve in the presence of MMA also followed the first-order kinetics. The apparent decay constants k_{ap} are shown in Figure (5.5) and can be written as

$$k_{ap} = k[MMA] + k_0, \qquad (5.2)$$

where [MMA] denotes the concentration of MMA. The rate constant k of the diphenylphosphinoyl radical with MMA was obtained as (2.2 ± 0.3) 10^7 mol^{-1} dm^3 s^{-1}. The rate constant of addition to MMA has been reported as (6.0 ±0.3) 10^7 mol^{-1} dm^3 s^{-1} by the transient absorption method.[1)] The values of the same order suggest that the same reaction process is reflected in the decay of transient absorption.

The decay of signal, which was accelerated in the presence of monomer, showed the single exponential. The first-order chemical reaction is reflected in the signal decay. As discussed in previous Chapters, the decay of signal is represented by equation (3.6) or equation (3.7). The apparent decay constant k_{ap} is the sum of reaction rate constants or the sum of reaction rate constants and the reciprocal of spin-lattice relaxation time. The observed relation of equation (5.1) and equation (5.2) can be interpreted according to equation (3.6) or equation (3.7).

In the present system, the initiation reaction of radical polymerization is directly observed by the time-resolved esr method. The rate constant of initiation is directly determined from the decay curves of esr signal.

5,4 Reactivity of the 2,4,6-trimethylbenzoyl radical

The time profiles of esr signal for the 2,4,6-trimethylbenzoyl radical without olefinic compounds and with olefinic compounds (0.5 mol dm^{-3}) are shown in Figure (5.6). As shown in Figure (5.1) and (5.3), the esr signal of the primary propagating radical due to the diphenylphosphinoyl radical superposed on the signal of the 2,4,6-trimethylbenzoyl radical. Thus, it is difficult to analyze the decay curves of signals. The decay curves, however, appeared to be not accelerated in the presence of olefinic compounds. No considerable effect of olefinic compounds exists on the decay curves, though the signal of the diphenylphosphinoyl radical was quenched at this concentration of olefinic compounds. It was indicated that the 2,4,6-trimethylbenzoyl radical did not react with olefinic compounds within the observed time region. Moreover, no propagating radical formed by the addition of the 2,4,6-trimethylbenzoyl radical to olefinic compounds was observed. The spin polarization relaxes before the initiation reaction, so that, the CIDEP signal of the primary propagating radical can not be detected. The 2,4,6-trimethylbenzoyl radical is less reactive than the diphenylphosphinoyl radical. The initiation can not be observed for the 2,4,6-trimethylbenzoyl radical by the time-resolved esr method, because of the low reactivity.

By the product analysis method, it has been reported that the diphenylphosphinoyl radical is more reactive than the 2,4,6-trimethylbenzoyl radical.[3] The initiation efficciency of the diphenylphosphinoyl radical was larger than that of the 2,4,6-trimethylbenzoyl radical. The present studies on these radicals

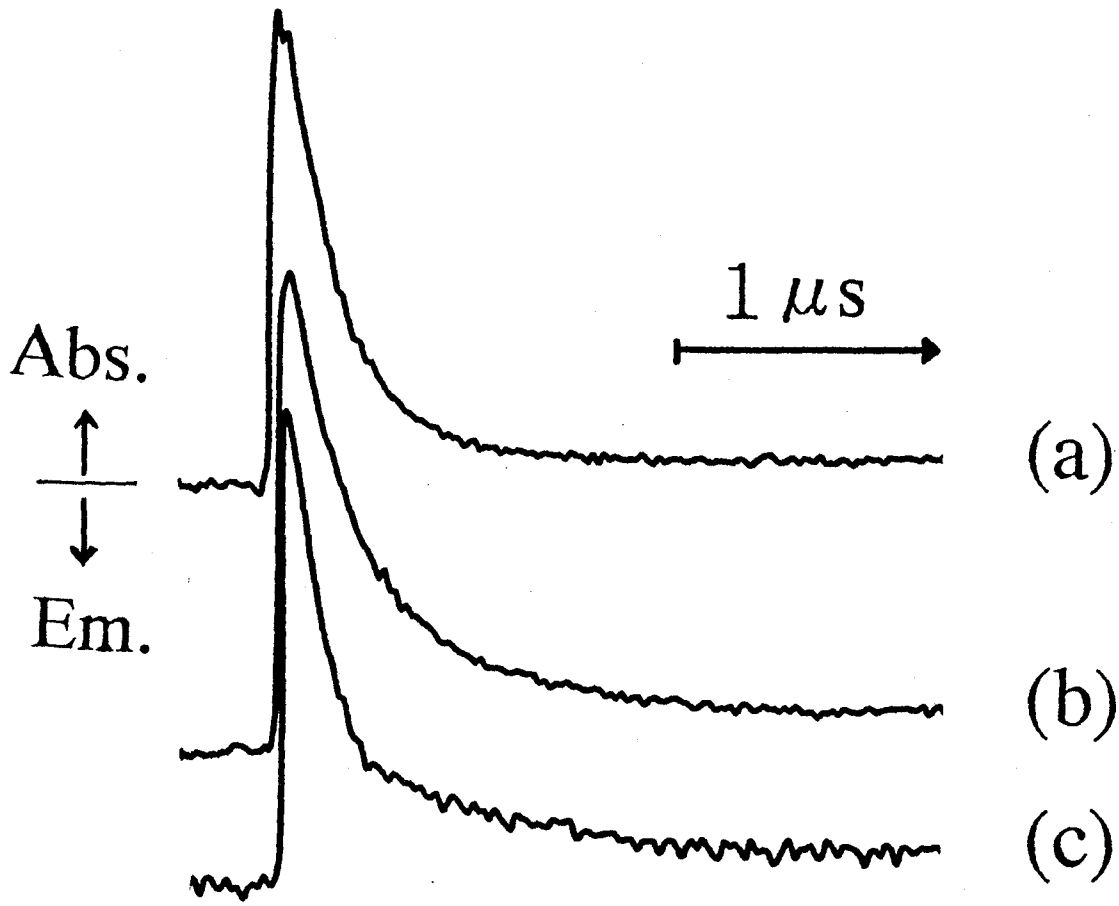

Figure (5.6) Time profiles of esr signal for the 2,4,6-trimethyl-benzoyl radical. (a) neat, (b) at the αMS concentration of 0.5 mol dm^{-3}, (c) at the MMA concentration, 0.5 mol dm^{-3}.

supported the result of product analysis.

Moreover, the 2,4,6-trimethylbenzoyl radical appears to be more susceptible to atomospheric oxygen in the product analysis experiments. In the present study, no oxygen effect was observed on the time-resolved esr signal of these fragment radicals. The radicals were not affected by oxygen in the observed time region. The signal of the diphenylphosphinoyl radical was quenched at the high concentration of olefinic compounds. Then, it can be concluded that the reaction of the diphenylphosphinoyl radical with monomer occurs sufficiently before the scavenging by oxygen at the high concentration of monomer. On the other hand, the reaction of the 2,4,6-trimethylbenzoyl radical is slow. Thus, the scavenging by oxygen can be significant. The result of the time-resolved study agrees with that of the product analysis in respect of the oxygen effect.

5.5 Substitution effect on the reactivity of the phosphinoyl radical

The signal decay of the di-*o*-tolylphosphinoyl radical followed the first-order kinetics. In the presence of MMA, the signal decay of the phosphinoyl radical was accelerated. The first-order decay constants k_{ap} are shown with the concentration of MMA in Figure (5.7) at the high field signal of the phosphinoyl radicals. The linear dependence of the decay constants k_{ap} on the concentration of MMA can be represented by equation (5.2). The rate constant k of the addition reaction for the di-*o*-tolylphosphinoyl radical with MMA was obtained to be 3.0 10^6 mol^{-1} dm^3 s^{-1}. The rate constant k of the di-*o*-tolylphosphinoyl radi-

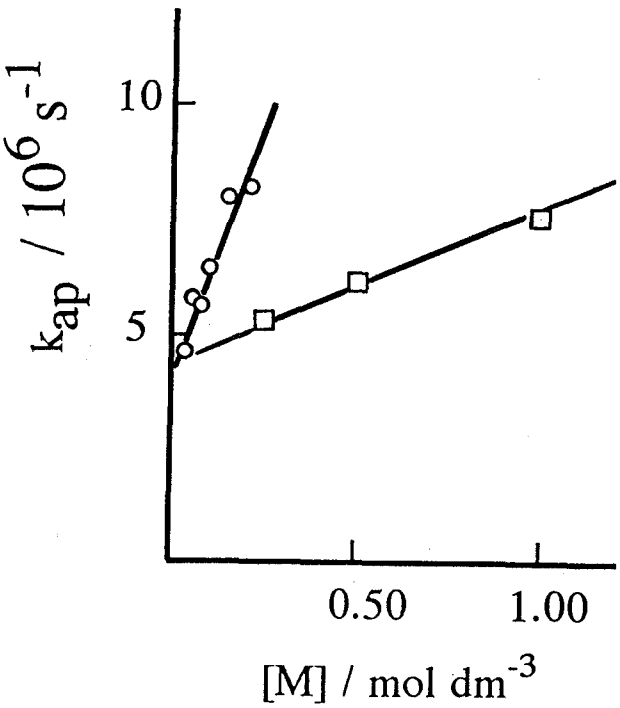

Figure (5.7) Dependence of the first-order decay constant k_{ap} of the phosphinoyl radicals on the MMA concentration at high field. ○: the diphenylphosphinoyl radical, □: the di-*o*-tolyl-phosphinoyl radical.

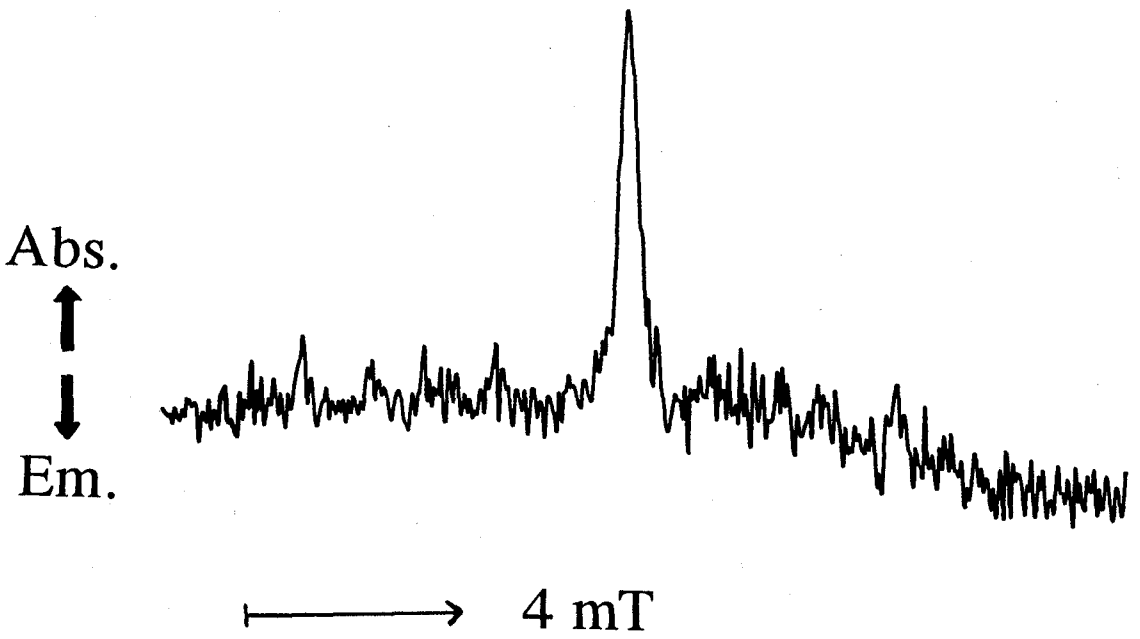

Figure (5.8) Time-resolved esr spectrum observed on the photolysis of TMTPO in the presence of MMA (0.5 mol dm^{-3}). Signal integration was carried out over the period between 200 ns and 400 ns after laser pulse.

cal was about ten times as small as that of the diphenylphosphinoyl radical. The substitution of aromatic protons at the ortho position by the methyl groups remarkably decreased the reactivity of the phosphinoyl radical with MMA.

The substitution effect to the reactivity of the phosphinoyl radical has been found by the transient absorption method.[2] The rate constants of the di-*o*-tolylphosphinoyl radical were about one order of magnitude lower than those of the diphenylphosphinoyl radical in the transient absorption experiment. The present study by the time-resolved esr method demonstrated the same result as the transient absorption method.

The difference of the reactivity in the phosphinoyl radicals is attributed to the steric factors. The time-resolved esr spectra, however, were almost the identical, as shown in chapter 4. The esr signals of the phosphinoyl radicals differed only in the decay rate in the presence of MMA. The substitution does not affect the structure of the radical with respect to esr spectrum.

The time-resolved esr spectrum observed on the photolysis of TMTPO in the presence of MMA is shown in Figure (5.8). In the case of the diphenylphosphinoyl radical, the spectrum of the product radical is shown in Figure (5.3). The product radical showed the total-absorptive signal of CIDEP due to the spin polarization transfer.[6] As shown in Figure (5.8), the esr signal of the product radical formed by the addition of the di-*o*-tolylphosphinoyl radical was remarkably weak in comparison with that of the diphenylphosphinoyl radical. (The central intense peak is due to the 2,4,6-trimethylbenzoyl radical.)

The polarization transfer is less effective due to the low

reactivity of the di-*o*-tolylphosphinoyl radical in the present case. The spin-lattice relaxation decreases the spin polarization in the transfer process. The chemical reaction should be sufficiently fast in comparison with relaxation for the observation of CIDEP in the product radical. In the case of the slow chemical reaction, the contribution of the relaxation is more significant than that of the fast chemical reaction. Thus, the esr intensity of the product radical would be small due to the low reactivity.

The substitution effect in the phosphinoyl radicals was found on the reactivity to MMA by the time-resolved esr method. The difference of rate constants was shown for the diphenylphosphinoyl radical and di-*o*-tolylphosphinoyl radical. TMDPO is more suitable as initiator than TMTPO, because of the high reactivity of the diphenylphosphinoyl radical. Moreover, in the present study, the primary propagating radical is observed by the time-resolved esr method. For this purpose, TMTPO is not suitable as sample initiator. TMDPO is a proper compound in the present work.

5.6 Photopolymerization with 2,2'-azobisisobutyronitrile (AIBN)

AIBN is frequently used as an initiator of radical polymerization. In polymerization of MMA by using of AIBN, the propagating polymer radicals have been detected by the steady-state esr measurement.[8] The primary propagating radical of monomer, however, could not be observed by the stady-state measurement.

Recently, the 2-cyano-2-propyl radical formed in the laser flash photolysis of AIBN has been detected by the time-resolved esr measurement.[10] The initiator radical shows the A/E pattern

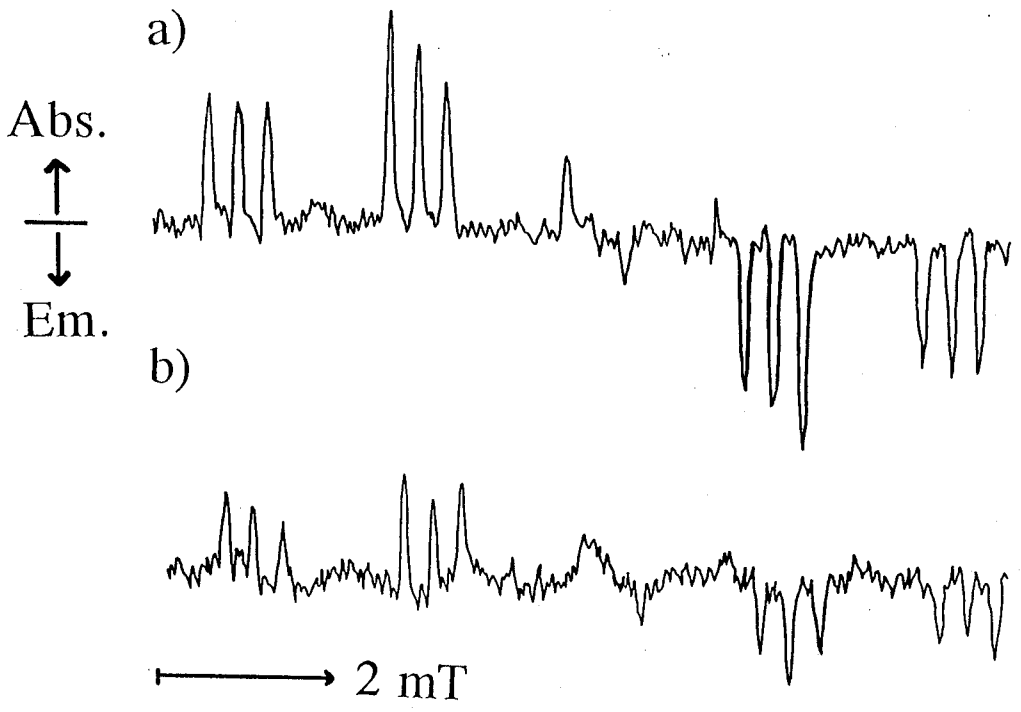

Figure (5.9) Time-resolved esr spectra of the 2-cyano-2-propyl radical in a) toluene and b) MMA. The concentration of AIBN is 0.2 mol dm^{-3}. Signal integration was carried out over the period between 200 ns and 400 ns after laser pulse.

spectrum due to the RPM of the S-precursor. In the present study, the time-resolved esr measurements were carried out on the toluene or the MMA solution of AIBN. The spectra which were obtained by using of the boxcar integrator over the period between 200 ns and 400 ns after laser pulse, are shown in Figure (5.9).

The signal of the 2-cyano-2-propyl radical was not quenched in the MMA solution. No considerable effect of MMA exists on the signal, and no product radical formed by the addition reaction was observed. Thus, the 2-cyano-2-propyl radical did not react with the MMA molecule in the observed time region. The rate of addition is much slower than that of the diphenylphosphinoyl radical. The addition reaction would occur slowly. This result indicates the low reactivity of the 2-cyano-2-propyl radical. The phosphorus-centred radical, such as the diphenylphosphinoyl radical, seems to have the higher reactivity of addition than the carbon-centred radical, such as the 2-cyano-2-propyl radical. The reaction process can not be observed in the addition of 2-cyano-2-propyl radical, because the spin polarization relaxes before the slow initiation reaction.

The 2-cyano-2-propyl radical did not show the total-absorptive (emissive) polarization, but the A/E pattern polarization. Then, the product radical formed by addition would not show CIDEP, if reaction rate was sufficiently fast. The spectrum of the product radical would not show the hfs due to the protons in the initiator moiety. In this case, the transfer of A/E pattern CIDEP can not occur. The polarizations of absorption and emission would cancel out in a esr line of the product radical. The

total-absorptive (emissive) polarization is necessary for the CIDEP detection of secondary radical in these case.

In radical polymerization, the initiation reaction occurs by the 2-cyano-2-propyl radical. The initiation step by AIBN, however, can not be observed by the time-resolved esr method. It is demonstrated that the proper initiator, such as TMDPO, is necessary for the observation of the initiation step by the time-resolved esr method.

References to chapter 5

1. (a) T.Sumiyoshi and W.Schnabel, Polymer, 26, 141(1985).
   (b) T.Sumiyoshi and W.Schnabel, Makromol. Chem. 186, 1811(1985).
2. T.Majima and W.Schnabel, J. Photochem. Photobiol., A, 50, 31(1989).
3. J.E.Baxter, R.S.Davidson, H.J.Hageman and T.Overeem, Makromol. Chem. 189, 2769(1988).
4. T.Sumiyoshi, W.Weber and W.Schnabel, Z.Naturforsch, Teil A, 40, 541(1985).
5. (a) R.Livingston, H.Zeldes and M.S.Conradi, J. Am. Chem. Soc. 101, 4312(1979).
   (b) D.R.Arnold, M.de P.Nicholas and M.S.Snow, Can. J. Chem. 63, 1150(1985).
6. (a) K.A.McLauchlan and N.J.K.Simpson, Chem. Phys. Lett. 154, 550(1989).
   (b) K.A.McLauchlan and N.J.K.Simpson, J. Chem. Soc. Perkin Trans 2, 1371(1990).
   (c) N.J.Turro and I.V.Khudyakov, Chem. Phys. Lett. 193, 546(1992).
   (d) K.Ohara, H.Murai and K.Kuwata, Bull. Chem. Soc. Jpn. 65, 1672(1992).
   (e) P.J.Hore and K.A.McLauchlan, Mol. Phys. 42, 533(1981).
7. (a) S.Brumby, J. Magn. Reson. 10, 203(1973).
   (b) W.Lung-min and H.Fisher, Helv. Chim. Acta. 66, 138(1983).
8. (a) P.Smith and R.Stevens, J. Phys. Chem., 76, 3141(1972).
   (b) P.Smith, L.B.Gilman and R.A.DeLorenzo, J. Magn. Reson., 10, 179(1973).

(c) M.Kamachi, Adv. Polym. Sci., 82, 207(1987), Springer-Verlag Berlin Heidelberg, and references therein.

9. M.Kamachi, K.Kuwata, T.Sumiyoshi and W.Schnabel, J. Chem. Soc. Perkin Trans 2, 961(1988).

10. T.Takemura, K.Ohara, H.Murai and K.Kuwata, Chem. Lett. 1635(1990).

6. Concluding Remarks

The evidences were obtained that the fragment radicals of TMDPO showed the absorptive CIDEP. The total-absorptive CIDEP is due to the TM in the photolysis of TMDPO. The triplet excited state of TMDPO, of which lifetime is extremely short, was the precursor of these radicals. No effect of oxygen was observed on the time-resolved esr spectrum. The possibility of thermal equilibrium were excluded on the esr signal of the diphenylphosphinoyl radical, of which the decay rate was independent of microwave power. The decay of signal can be due to both chemical reactions and the decay of CIDEP. The signal at the thermal equilibrium state was found to be negligible. It is demonstrated that polarization transfer, triplet quenching and effect of relaxation reagent are useful to analyze the time-resolved esr signal.

On the photolysis of TMDPO and TMTPO, the substitution of aromatic protons at the ortho position by the methyl group did not affect the time-resolved esr spectra of the phosphinoyl radicals.

On the photolysis of the acylphosphine sulphides, the E^*/A spectra of the thiophosphinoyl radicals were observed. The radicals ar

formed from the triplet excited state. The intense signal due to the TM, however, was not observed. The emissive contribution in spectra were dependent on the viscosity of solvent. Thus, it is concluded that the contribution of CIDEP due to the ST_mixing exists in the spectra. The mechanism of CIDEP of the 2,4,6-trimethylbenzoyl radical is not identified on the photolysis of TMTPS.

It was found that the decays of esr signal for the diphenylphosphinoyl radical was accelerated in the presence of olefinic compounds . The second-order rate constants of addition reaction with the olefinic compounds were determined from the analysis of the decays, and the value close to that of the transient absorption measurement was obtained. The product radicals due to the addition reaction of the diphenylphosphinoyl radical with olefinic compounds were observed by the time-resolved esr measurement and their esr signal showed CIDEP. For the 2,4,6-trimethylbenzoyl radical, the esr signal did not change in the presence of olefinic compounds. The 2,4,6-trimethylbenzoyl radical is less reactive than the diphenylphosphinoyl radical. It is the same result as the product analysis experiment. The reactivity to olefinic monomer was remarkably decreased and the decay curve of esr signal is affected by the substitution in the phosphinoyl radicals. The product radical from the di-*o*-tolylphosphinoyl radical is not clearly observed due to the slow reaction. The addition reaction of 2-cyano-2-propyl radical could not be observed in the photolysis of AIBN by the time-resolved esr method. In the present studies, the reaction of transient radicals is observed and the reactivities of radicals were discovered by the time-resoled esr method.

The initiation step was directly observed in the photopolymerization system with the time-resolved esr method. The initiator radicals were detected and the CIDEP was examined. The addition reaction of initiator radical was observed. The primary propagating radical could be observed due to the polarization

transfer. The rate constant of initiation was determined from the decays of esr signal. The observation can be carried out due to the total-absorptive CIDEP and the high reactivity of the diphenylphosphinoyl radical. The application of the time-resolved esr spectroscopy is demonstrated to the study on photopolymerization in the present work.

7. Acknowledgment

The author would like to his gratitude to Professor Keiji Kuwata of Osaka University for guidance and research advice in Osaka University and helpful suggestion and kind encouragement in preparation of the present thesis.

The author would like to express his gratitude to Professor Mikiharu Kamachi of Osaka University for advice, suggestion and encouragement. The author would like to acknowledge Professor Wolfram Schnabel of Hahn-Meitner Institut and Dr. Tetsuro Majima of Institute of Physical and Chemical Research for sample donation and helpful suggestion. The author would like to acknowledge Dr. Hisao Murai of Osaka University for helpful suggestion and encouragement. The author would like to express his gratitude to Dr. Masaharu Okazaki and Dr. Kazumi Toriyama of Government Industrial Research Institute Nagoya for encouragement in preparation of the present thesis.